Response to interactive comments for:

Seafloor geomorphology of western Antarctic Peninsula bays: a signature of ice flow behaviour

We want to thank the reviewers and the editor for their constructive and insightful comments. We have made revisions to the manuscript based on the comments provided by the referees. The annotated document with track changes is tc-2017-108-AC1-supplement. Below are answers to specific reviewers' comments followed by the revised manuscript with track changes (underlined are the reviewer comments, followed by the author comments in red).

C. Stokes:
Include 1) a much clearer and explicit presentation of the mapped data, 2) a clearer and more objective separation of the results from the interpretations, and 3) a more in-depth and critical analysis in the discussion.

Y. Munoz:
1) We have included interpretation maps for all the bays mentioned in this paper. In addition, we have included a table describing the criteria used for identifying the features mentioned in the study and we have annotated Fig. 6 which shows examples of the seafloor features mapped.
2) The results have been clearly separated from the interpretations. Results only describe the geomorphology present in the bays as well as geometries of landforms, and interpretation of these landforms is now in the first section of the discussion.
3) The discussion section has been modified to include the interpretation of geomorphic features and some sub-sections have been removed to avoid repetition.

A.G.C. Graham:
1) the authors might want to consider their method and whether it is still adequate to simply present sea-floor data without a clear and objective mapping of the landforms alongside.
We agree, we have included interpretation maps of all the bays presented in this paper.

2) a clearer separation of the descriptions and interpretations of the landforms in the results section
In the revised manuscript, results include only descriptions. Interpretations are listed under discussion.

3) some of the interpretations themselves need some better explanation supported by more in-depth analysis and relevant literature
We have tried to clearly separate features and include more relevant literature for the interpretation.

4) Some of the multibeam observations might also be better supported by a closer integration and more widespread study of sub-bottom profiler data
Unfortunately, we do not have subbottom profiler data paired with the multibeam data. We only have CHIRP data from one cruise, compared to the seven cruises from which we have multibeam data. The CHIRP has been loaded into a project in Kingdom Suite, where we tried applying some filters to clean the data and the results are shown in Figure 7. Given limited areal extent of the data, we did not create lithology maps of the bays.

5) I remain a little unconvinced by the correlation of landform number to bay size. It seems logical to me that smaller fjords will contain fewer landforms than larger ones

We agree, this is intuitive but we still include the correlation because we are also comparing glacier catchment area, and we are suggesting that glacier catchment area does not directly correlate with the number of features regardless of the size of the bay.

6) The LIA discussion is interesting but I felt under-developed. Is it feasible to form a fjord GZW of the sizes you are observing during and since the LIA, based on what you know about sediment fluxes? Why are these all LIA age when Fig 12i clearly shows one of the wedges at least to lie coincidental with a mid-20th century glacier front position?

Boldt et al. is one of the few publications that have sedimentation rates for the bays we show in this paper. In several of these bays there are no published sedimentary records and therefore we are inferring deglaciation based on geomorphology alone. Because the proximal area in Barilari Bay (Christ et al.) is very similar to other bays, we assume they may have formed by the same event. But we agree that in some cases, the ice front mapped by Cook et al. coincides with some of the transverse landforms, and these may be younger than LIA. We have included this statement as an alternative idea in the LIA section.

S.J. Livingstone:

1) this paper would be considerably stronger if the authors could present the mapping results of their work as a series of maps

We agree, we now show mapping results for the bays.

2) there is no clear rationale of how the authors identified the glacial features and interpreted them

We have included a table describing the criteria used for identifying the features mentioned in the study and we have annotated Fig. 6 which shows examples of the seafloor features mapped.

3) some sections lack thorough characterisations of the glacial features (e.g. length, width, shape). Some results and interpretations are mixed up.

We have added geometric information of the landforms as detailed as possible in results and the criteria table. We also separated the description (results) from the interpretation of these glacial features.

4) CHIRP needs to come in the results

We have included the CHIRP data in the results, however there is limited coverage and in some areas there are no CHIRP data. The section on seafloor lithology has been removed from the discussion and merged with the results to better characterize the features.

5) Meltwater channels. In the discussion, you distinguish between proglacial, postglacial and subglacial channels, but it is not clear what evidence you base this on

Meltwater channels have been separated into subglacial and proglacial, and in the discussion, we describe the reasoning behind this interpretation.

6) The section of basin area and catchment area (and length and width too) is weak

We agree that the results of this section are intuitive. We still include the correlation because we are also comparing glacier catchment area, and we are suggesting that glacier catchment area does not directly correlate with the number of features regardless of the size of the bay.

7) The data you have on moraine/GZW positions is nice, but I think more could be made of it. Why not compile data on their size and where they occur?

We include size of moraines and GZW in the identification criteria table. We also describe where they occur in the discussion section.

Additional referees' comments in the annotated PDF are not included in this text, but are addressed in the revisions of the manuscript.

The introduction has been modified to explain that this paper is focused in four bays along the Antarctic Peninsula but we integrate data from other 7 locations to support our results. The multibeam maps and the interpretation of features for these 7 locations are included in the supplementary material.

Regional setting has been changed to Study Area to include a short introduction to each one of the four bays and climate in the area.

The discussion section has been modified. We no longer include the category "landforms formed by glacial retreat and minor re-advances", these features have been distributed to either "subglacial", "ice-marginal" or "recent sediment reworking" category. The sections on water depth and seafloor lithology have been removed from "Observations on flow dynamics" to avoid repetition.

Seafloor geomorphology of western Antarctic Peninsula bays: a signature of ice flow behaviour

Yuribia P. Munoz[1], Julia S. Wellner[1]

[1]Department of Earth and Atmospheric Sciences, University of Houston, Houston, Texas 77204 USA

Correspondence to: Y.P. Munoz (ypmunoz@uh.edu)

Abstract. Glacial geomorphology is used in Antarctica to reconstruct ice advance during the Last Glacial Maximum and subsequent retreat across the continental shelf. Analogous geomorphic assemblages are found in glaciated fjords and are used to interpret the glacial history and glacial dynamics in those areas. In addition, understanding the distribution of submarine landforms in bays and the local controls exerted on ice flow can help improve numerical models by providing constraints through these drainage areas. We present multibeam swath bathymetry from several bays in the South Shetland Islands and the western Antarctic Peninsula. The submarine landforms are described and interpreted in detail. A schematic model was developed showing the features found in the bays; from glacial lineations and moraines in the inner bay, to grounding zone wedges and drumlinoid features in the middle bay, and streamlined features and meltwater channels in the outer bay areas. In addition, we analysed local variables in the bays and observe that: 1) the number of landforms found in the bays scales to the size of the bay, however, the geometry of the bays dictates the types of features that form, specifically, we observe a correlation between the bay width and the number of transverse features present in the bays; 2) the smaller seafloor features are present only in the smaller glacial systems indicating that short-lived atmospheric and oceanographic fluctuations, responsible for the formation of these landforms, are only recorded in these smaller systems; and 3) meltwater channels are abundant on the seafloor, however some are subglacial, carved in bedrock, and some are modern erosional features, carved on soft sediment. Lastly, based on geomorphological evidence, we propose the features found in some of the proximal bay areas were formed during a recent glacial advance, likely the Little Ice Age.

Deleted: has been
Deleted: during the Last Glacial Maximum
Deleted: can be
Deleted: in a similar manner
Deleted: ice-sheet
Deleted: complicated
Deleted: flutings
Deleted: s
Deleted: bay length and width exert a control on the
Deleted: ,
Deleted: ~~2) bays with shallower water depths tend to form geomorphic features that suggest rapid decoupling of grounded ice from the seafloor;~~ 3
Formatted: Strikethrough
Deleted: 4
Deleted: inner

1 Introduction

While warming temperatures in the Antarctic Peninsula (AP) have resulted in the retreat of 90% of the regional glaciers (Cook et al., 2014) and the collapse of ice shelves (Morris and Vaughan, 2003; Cook and Vaughan, 2010), recent studies have shown that since the late 1990s this region is currently experiencing a cooling trend (Turner et al., 2016). The AP is a dynamic region that serves as a natural laboratory to study ice flow and the resulting sediment deposits. As the ice retreats, it leaves behind glacial geomorphic features on the seafloor; these submarine landforms have been mapped in glaciated environments in Antarctica (Anderson et al., 2001; Wellner et al., 2001; Evans et al., 2004; Heroy and Anderson, 2005;

Deleted: since the late 1990s
Deleted: flows
Deleted: other

Wellner et al., 2006; Larter et al., 2009; Livingstone et al., 2013; Hodgson et al., 2014), southern Chile (Dowdeswell and Vasquez, 2013), North America (Dowdeswell et al., 2016) and northern Europe (Ottesen et al., 2005; Ottesen and Dowdeswell, 2006; Ottesen and Dowdeswell, 2009; Dowdeswell et al., 2010) giving insight into the glacial history of each region. Several seafloor features have been mapped west of the AP on the continental slope and continental shelf (Dowdeswell et al., 2004; Graham and Smith, 2012; Gales et al., 2013), the South Shetland Islands (Milliken et al., 2009; Simms et al., 2011), South Georgia Island (Hodgson et al., 2014; Graham et al., 2017), Bransfield Strait (Canals et al., 2000; Canals et al., 2002), Gerlache Strait (Evans et al., 2004), south of Anvers Island (Domack et al., 2006) and Marguerite Bay (Ó Cofaigh et al., 2002; Anderson and Fretwell, 2008; Livingstone et al., 2013). However, the seafloor geomorphology in western AP bays has not been described in detail, except for a few locations (Garcia et al., 2016; Munoz and Wellner, 2016; Wolfl et al., 2016). Although most of the data we present is publicly available, this is the first instance, to our knowledge, that a detailed description of the seafloor geomorphology of a large number of western AP fjords has been completed.

Deleted: in

Deleted: publically

Deleted: where

We combine multibeam swath bathymetry data collected during seven cruises to the Antarctic Peninsula. The multibeam bathymetry data presented in this study expose geomorphic features formed during past ice flow in several bays in the western Antarctic Peninsula, the South Shetland Islands, and Anvers Island (Fig. 1). We focus this study on four bays throughout the AP: Maxwell Bay, located on King George Island (KGI), north of the AP; Hope Bay, located on the northernmost tip of the AP known as the Trinity Peninsula; Lapeyrère Bay, on Anvers Island, west of the AP; and finally, Beascochea Bay, located in the Graham Land Coast of the western AP (Fig. 1). Data from additional bays throughout the AP (found in supplementary material) have been integrated in the results section to support this investigation. The glacial seafloor features reveal flow behaviour of grounded ice; structures formed in a deformable sedimentary substrate likely represent subglacial conditions shortly before ice decoupling from the seafloor, and structures in bedrock likely formed over several glacial-interglacial cycles (Wellner et al., 2001; Campo et al., 2017). We map the glacial landforms and analyse local variables including bay length and width, glacier drainage size flowing into the bays, seafloor lithology, and water depth in order to understand the controls of ice flow and retreat dynamics in these locations.

Deleted: present

Deleted: geomorphic features

Deleted: on the seafloor of various bays

Deleted: each

Deleted: . Although we do not provide any age constraints, submarine landforms are used to interpret relative timing of deglaciation in the bays.

2 Study Area

Deleted: Regional

Deleted: Setting

The AP is the northernmost extent of the Antarctic continent. The AP is a long (~1200 km), thin (~250 km) strip of mountains of up to 3500 m in elevation. The geological setting of the AP is characterized by Cenozoic tectonic extension and active volcanism (Griffith and Anderson, 1989). Glacial ice flow over crystalline bedrock has preferentially eroded over joints and faults, accentuating their appearance (Domack et al., 2006). The predominant rock types are metamorphic and intrusive and extrusive igneous rocks (Griffith and Anderson, 1989). Ice covers about 80% of the AP, where ice thickness ranges between 400 to 800 m (Fretwell et al., 2013) and averages about 500 m. The ice cap covering Anvers Island reaches up to 600 m, similar to the western AP (Ashley and Smith, 2000), while in King George Island, the ice cap is only 150-200 m thick (Simms et al., 2011).

The high peaks of the AP form a topographic barrier to the westerly winds resulting in a warmer, wetter western AP, and a cooler, dryer eastern AP (Ó Cofaigh et al., 2014). The climate in Hope Bay (northern AP, Fig. 1) is cold, dry semi-polar (Pereira et al., 2013). Annual air temperature at Esperanza Research Station (located in Hope Bay) range between -30.6° C and 11.8° C, with an average of -5.1° C, and an annual precipitation of 250 mm measured between 1952 and 2010 (Pereira et al., 2013; Schaefer et al., 2016). In contrast, the western AP receives an average of 1100 mm yr^{-1}, measured between 1997 and 2006 (Thomas et al., 2008), and up to 2900 mm yr^{-1} in some bays (Fernandez et al., 2016). Annual air temperatures in the western AP vary between slightly above 0° C in the summers to -8° to -11° C in the winters (King et al., 2003). Sea ice covers the bays seasonally, but most areas are sea-ice free during the summers (Domack and Ishman, 1993). The islands experience a maritime climate. KGI has a temperate to sub-polar glacial setting (Yoon et al., 2004), with little changes in air temperature throughout the year (average of -1.8° C, minimum of -5.7° C in July, and maximum of 2° C in January). Mean annual precipitation is about 1200 mm on the higher elevations, but much less in areas like Potter Cove where precipitation data indicate an annual average of 524 mm (Lee et al., 2008; KOPRI, 2014; Moon et al., 2015; Fernandez et al., 2016). In Anvers Island (west of the AP, Fig. 1), summer air temperatures reach up to 6-7.5° C, while in the winter is -5° C on average (Ashley and Smith, 2000). Precipitation in Anvers Island is on average approximately 1200 mm annually (Griffith and Anderson, 1989; Ashley and Smith, 2000) and up to 2000 mm yr^{-1} in Lapeyrère Bay, northern Anvers Island (Fernandez et al., 2016).

2.1 Maxwell Bay

Maxwell Bay (62°13.7'S, 58°50.9'W) (Fig. 2) is located in the western end of King George Island. Maxwell Bay is about 15 km long and between 6-15 km wide, and has an approximate area of 140 km^2. Maxwell Bay has several embayments; Edgell Bay, Ardley Harbor, Collins Harbor, Marian Cove (Fig. 2b), and Potter Cove (Fig. 2c). Water depths vary widely from 35 m in the inner bay to 500 m in the outer bay. The outer bay is U-shaped (Fig. 2, C-C'), with tens of meters of sediment cover (Milliken et al., 2009; Fernandez et al., 2015). The glacier catchment area around Maxwell Bay is about 92 km^2, separated into four discrete glaciers. Collins Harbor, north end of Maxwell Bay, has a sediment accumulation rate of 5.5 mm yr^{-1} (Boldt et al., 2013).

Marian Cove (62°12.8'S, 58°46.1'W) (Fig. 2b) is an elongated bay in northeastern Maxwell Bay. The bay is approximately 4 km long and between 1-1.5 km wide, with an approximate area of 5 km^2. A single tidewater glacier (with a catchment area of about 15 km^2) drains directly into the bay. This glacier retreated about 1.7 km between 1956 and 2013 (Lee et al., 2008; Moon et al., 2015). Large meltwater and sediment influx into the bay occur in the summer months (Moon et al., 2015). Sediment accumulation rates vary between 5.2 and 6.6 mm yr^{-1} in Marian Cove (Boldt et al., 2013).

Formatted: Normal
Formatted: Font: Bold
Moved (insertion) [1]
Deleted: (Fig. 4)
Deleted: Potter Cove (Fig. 4b) and
Deleted: (Fig. 4c)
Deleted: formed by
Deleted: ¶

Potter Cove (62°13.9'S, 58°41.2'W) (Fig. 2c) is an elongated bay in southeastern Maxwell Bay. Potter Cove is approximately 4 km long and between 1 km wide in the bay head and 2.5 km wide in the bay mouth, approximately 7 km^2 in total area, and with water depths ranging between 25-150 m. Fourcade Glacier drains directly into this bay, however most of it terminates on land. The glacier catchment area is about 20 km^2. Ice front retreat of Fourcade Glacier has been approximately 1 km in Potter Cove between 1956 and 2008 (Wolfl et al., 2016), with a greater retreat of grounded ice in the tidewater part of glacier and much less on the land-based grounded ice (Ruckamp et al., 2011). Meltwater discharges are common in Potter Cove, especially during the summer (Wolfl et al., 2014), with sediment accumulation rates in outer Potter Cove of 1.6 mm yr^{-1} (Boldt et al., 2013).

2.2 Hope Bay

Hope Bay (63°24.4'S, 57°2.8'W) (Fig. 3) is located along the northernmost tip of the Antarctic Peninsula, draining into the Antarctic Sound. The bay is 6 km long, and between 800 m wide in the bay head and 3 km wide in the bay mouth; the bay area is about 11.5 km^2. Water depths in Hope Bay vary between 50-320 m. Two large glaciers drain directly into the bay; Depot Glacier (catchment area of 7 km^2) and Arena Glacier (catchment area of 16 km^2). In addition, three unnamed glaciers (each with an average area of 3 km^2) also discharge into Hope Bay. Boldt et al. (2013) measured a sediment accumulation rate of 3 mm yr^{-1} in Hope Bay.

2.3 Lapeyrère Bay

Lapeyrère Bay (64°25.3'S, 63°17'W) (Fig. 4) is located in northeastern Anvers Island. Lapeyrère Bay is a narrow, elongated bay with water depths varying from 250-740 m. The bay is 11 km long, 2 km wide in the bay head and 3.5 km in the bay mouth, with an overall bay area of 32 km^2. One large glacier, Iliad Glacier (catchment area of 234 km^2), drains into the bay, in addition to other smaller glaciers around the perimeter of the bay, each with an average catchment area of 6 km^2. Sediment accumulation rates in Lapeyrère Bay are 2.2-3.2 mm yr^{-1} (Boldt et al., 2013).

2.4 Beascochea Bay

Beascochea Bay (65°31'S, 63°52.2'W) (Fig. 5) is the southernmost bay presented in this study. It is an elongated bay with several embayments in the bay head, three of them described below. Each one of the described embayments has a large glacier draining directly into it. None of the coves are named and therefore, for the purposes of this paper, we use the name of the glacier to identify the cove; Lever Glacier Cove, Funk Glacier Cove, and Cadman Glacier Cove. Beascochea Bay is approximately 24 km long, 6-13 km wide, with an approximate bay area of 235 km^2. Several glaciers drain into this bay along its perimeter; their individual catchment area varies between 1-28 km^2. Sediment accumulation rates in Beascochea Bay vary between 2.2 and 7 mm yr^{-1} (Boldt et al., 2013).

Moved (insertion) [2]

Deleted: (Fig. 4b)

Deleted: the

Deleted: edge of

Deleted: . Potter Cove has a small area compared to Maxwell Bay, only

Deleted:

Deleted: o

Deleted: on land

Formatted: Font: Not Bold

Deleted: ¶
Marian Cove (62°12.8'S, 58°46.1'W) (Fig. 4c) is an elongated bay, in the northeastern edge of Maxwell Bay, north of Potter Cove. The bay is approximately 4 km long and between 1-1.5 km wide, with an approximate area of 5 km^2. A single tidewater glacier (with a catchment area of about 15 km^2) drains directly into the bay. It is worth noting that this glacier retreated about 1.7 km between 1956 and 2013 (Lee et al., 2008; Moon et al., 2015). Large meltwater and sediment influx into the bay occur in the summer months (Moon et al., 2015). ¶

Moved (insertion) [3]

Formatted: Font: Bold

Moved (insertion) [4]

Deleted: (Fig. 5)

Deleted: in

Deleted: , in an area known as Trinity Peninsula

Deleted: and

Deleted: s out

Deleted: other

Deleted: small,

Deleted: drain

Deleted: ¶

Formatted: Font: Bold

Formatted: Font: Bold

Moved (insertion) [5]

Deleted: (Fig. 6)

Deleted: , and shallowing towards the fjord walls

Formatted: Font: Bold

Formatted: Superscript

Lever Glacier cove (65°30.7'S, 63°43.4'W) (Fig. 5b) is an elongated bay, 6 km long and 3 km wide, with a total bay area of about 16 km^2. The largest glacier draining into this cove is Lever Glacier (catchment area of 177 km^2), other glaciers draining into the bay are much smaller (individual average area is about 4 km^2). Funk Glacier cove (65°34.8'S, 63°45.4'W) (Fig. 5c) is an elongated bay, 4 km long and 2 km wide, with a total bay area of about 8 km^2. A large glacier drains directly into this cove, Funk Glacier, with a surface area of 158 km^2. Another small glacier, with a surface area of 3 km^2, also flows into the cove. During the late 1960s, this cove was covered by ice (Cook et al., 2014). Although it is unclear whether the ice cover was grounded ice or permanent sea ice, the fact that this area has alternated between ice-free and ice-covered since the late 1960s suggests fast sea ice cover and not grounded ice. Cadman Glacier cove (65°36.7'S, 63°48.7'W) (Fig. 5c) is the smallest cove surveyed in Beascochea Bay; it is 3 km long and 3 km wide, the total bay area is about 9 km^2. One large glacier drains directly into this cove, Cadman Glacier, with a surface area of 307 km^2.

3 Methods

Multibeam swath bathymetry data were collected on multiple research expeditions to the western AP aboard the RV/IB *Nathaniel B. Palmer* (NBP0201, NBP0502, NBP0602A, NBP0703, NBP1001, and NBP1203) and the RV/IB *Araon* (ARA1304). Multibeam soundings were collected in a swath perpendicular to the ship track using a hull-mounted Kongsberg EM120 multibeam echosounder, with a swath of 191 beams, operating at a frequency of 12 kHz on the NBP cruises and Kongsberg EM122, with a swath of 432 beams, operating at a frequency of 12 kHz on the ARA cruise. These data sets were merged using CARIS HIPS & SIPS where the survey data were manually edited to remove anomalous readings and gridded to create relief maps. Grids were created per bay at resolutions of 25 m and in some cases 10 m. Here we show the optimal resolution of the data, which in most cases is the 25-m grid. These grids were then imported into ArcGIS 10 where hillshade effect was created with a z-factor >1 to simulate vertical exaggeration. This compilation of bathymetry in addition to other data sets have recently been published in Boldt et al. (2013) and Lavoie et al. (2015). In addition to mapping the submarine landforms, we compare them to the local physiographic variables of each bay including latitude, area, length, width, glacier catchment area, and the seafloor lithology based on CHIRP results, to understand controls on ice flow behaviour. High resolution shallow subbottom CHIRP profiles were collected during NBP0703 throughout the study area. The data were collected using a hull-mounted Knudsen 320B/R with a frequency of 3.5 kHz and it has been interpreted using SMT Kingdom software. CHIRP sonar provides a vertical resolution of about 1 m and can image unconsolidated sediments up to 100 m below the seafloor. The CHIRP data were used to identify seafloor lithology (sediment type or bedrock) and the thickness of sedimentary units.

Moved (insertion) [6]

Deleted: **Beascochea Bay (65°31'S, 63°52.2'W) (Fig. 7) is the southernmost bay presented in this study. It is an elongated bay with several embayments in the bay head, three of them are described below. Each one of the described embayments has a large glacier draining directly into it. None of the coves are named and therefore, for the purposes of this paper, we use the name of the glacier to identify the cove; Lever Glacier Cove, Funk Glacier Cove, and Cadman Glacier Cove. Beascochea Bay is** approximately 24 km long, 6-13 km wide, **with an approximate bay area of 235 km^2. Several glaciers drain into this bay along its perimeter; their individual catchment area varies between 1-28 km^2.** ¶

Moved (insertion) [7]

Deleted: (Fig. 7b)…is an An …longated bay, 6 km long and 3 ...

Formatted: Font: 10 pt

Moved (insertion) [8]

Deleted: (Fig. 7c) is an An …longated bay, 4 km long and 2 km ...

Moved (insertion) [9]

Deleted: (Fig. 7c) This cove ...

Deleted: ,

Deleted: ¶
¶
2.1 King George Island¶
The northernmost study area is Maxwell Bay, located in King George Island, the largest island of the South Shetland Islands (SSI) archipelago. The SSI are separated from the AP by the Bransfield Strait (Fig. 1). The region has a temperate to sub-polar glacial setting (Yoon et al., 2004). King George Island experiences a maritime climate, with little changes in air temperature throughout the year (average of -1.8° C, minimum of -5.7° C in July, and maximum of 2° C in January), mean annual precipitation of 1249 mm, with high summer rain and high relative humidity (average 88.7%) (Lee et al., 2008; KOPRI, 2014; Moon et al., 2015; Fernandez et al., 2016). King George Island is covered by an ice cap (approximately 150-200 m thick), and Maxwell Bay has rocky to gravelly beaches (Griffith and Anderson, 1989; Simms et al., 2011). Sediment accumulation rates vary throughout Maxwell Bay: 5.5 mm yr^{-1} in inner Collins Harbor, 5.2-6.6 mm yr^{-1} in inner Marian Cove, and 1.6 mm yr^{-1} in outer Potter Cove (Boldt et al., 2013). The rock outcrops in the island include upper Jurassic volcanic rocks, lower Tertiary to upper Cretaceous Andean intrusive rocks (including adamellite, diorite, granite, gabbro, granodiorite, quartz diorite, and tonalite), upper Tertiary volcanic rocks, Pliocene conglomerates and Quaternary volcanic rocks (Adie, 1969).¶
¶
2.2 Trinity Peninsula¶
The northernmost tip of the AP is known as the Trinity Peninsula (Fig. 1). Pereira et al. (2013) classified the climate of Hope Bay (located on the northern tip of the AP) as cold, dry semi-polar. Annual air temperature at Esperanza Research Station (located in front of the Antarctic Sound) have been measured to range between -30.6° C and 11.8° C, with an average of -5.1° C, and an annual ...

Formatted: Font: Not Bold, Font color: Auto, English (United States)

Deleted: on aboard the RV/IB *Nathaniel B. Palmer* (NBP0201, ...

4 Bathymetry Results

We describe the seafloor landforms identified in the bays of the western AP. Figure 6 shows some of these individual landforms mapped on the seafloor and Table 1 lists the criteria for identification in this study. The interpreted CHIRP facies are shown in Fig. 7. Maps of interpreted seafloor features throughout individual bays are shown in Figures 2-5 and in the supplementary material. In addition, data tables in the supplementary material show the bay location, length, width, area, number of glaciers in each bay, total glacier catchment area, and the submarine landforms found in each bay.

4.1 Maxwell Bay

The seafloor in northern Maxwell Bay (Fig. 2), near Collins Harbor and Ardley Harbor, is a large, shallow platform with water depths up to 280 m. Water depths increase rapidly to >400 m in the middle of the bay, where gullies and channels that cut into the seafloor can be found. Meltwater channels (1-4 km long, 10-30 m wide, and 1-2 m deep) are present on the seafloor from Edgell Bay and from Marian Cove trending towards the middle of Maxwell Bay. Large promontories are located between King George Island and Nelson Island. A few elongated hills, parallel to the bay axis, are present in the middle of the bay (Fig. 2, B-B'). These seamounts range in length 1-2.5 km, maximum width of 200-800 m and a maximum height of 10-50 m. Sediment thickness in the outer bay are in excess of 100 m (Milliken et al., 2009), and therefore other features carved by flowing ice in this area, if any, are buried. Simms et al. (2011) described a large sediment fan at the mouth of Maxwell Bay, draining out of the bay into the Bransfield Strait. The fan has a sediment thickness of up to 1000 m and it is located in water depths between 400 and 1400 m.

The seafloor topography of Marian Cove (Fig. 2b) is characterized by transverse ridges in the bay (Fig. 2, D-D'). Three major transverse ridges divide the bay into a proximal, middle, and outer basin. The proximal basin is the deepest, up to 135 m depth compared to 120 m and 110 in the middle and outer basin, respectively. The outer, most distal transverse ridge separates Marian Cove from Maxwell Bay. This feature is at least 650 m long, 200 m wide, and 20 m high. Although this feature is found across the width of the bay, water depth varies along the ridge crest from 40 m in the north to 70 m in the south. The middle ridge (approximately 1 km long, 100 m wide, and 8 m high) appears breached, with a possible slope failure deposit located on the west side of the ridge. Unfortunately, the resolution of the data is not clear enough to fully resolve this feature. However, the deposits have a fan shape and the water depths are shallower in this area indicating a likely mass wasting deposit. The inner, most proximal ridge (approximately 500 m long, 300 m wide, and between 20-30 m high) is wider than the other two and it could possibly be an amalgamation of more than one ridge. The data show hints of other, smaller ridges across the bay, located between the larger ridges, but these are not resolved due to the low resolution of the data. The inner (most proximal) basin seafloor shows elongated (80-340 m long), narrow hills (10-35 m wide, 1-2 m high), parallel to the bay axis, unevenly-spaced. Lastly, a topographic high, about 250 m long, 200 m wide, and 15 m high is

Deleted: found

Deleted: Antarctic Peninsula

Deleted: 2

Deleted: features

Deleted: in

Deleted: Fig. 3 shows t

Deleted: interpreted

Deleted: Below we describe the seafloor geomorphology in four bays in the western AP; maps and cross sections of the other bays in this study can be found in the supplementary material. D

Deleted: latitude, longitude

Deleted: , bay

Deleted: and

Deleted: bay

Deleted: **King George Island-**

Moved up [1]: Maxwell Bay (62°13.7'S, 58°50.9'W) (Fig. 4) is located in the western end of King George Island. Maxwell Bay is about 15 km long and between 6-15 km wide, and has an approximate area of 140 km^2. Maxwell Bay has several embayments; Edgell Bay, Ardley Harbor, Collins Harbor, Potter Cove (Fig. 4b) and Marian Cove (Fig. 4c). Water depths vary widely from 35 m in the inner bay to 500 m in the outer bay. The outer bay is U-shaped, with tens of meters of sediment cover (Milliken et al., 2009; Fernandez et al., 2015). The glacier catchment area around Maxwell Bay is about 92 km^2, formed by four glaciers.¶

Deleted: ¶

Deleted: forming

Deleted: in this area of Maxwell Bay

Deleted: Long channels

Deleted: , presumably active,

Deleted: observed

Deleted: flowing

Deleted: and are possibly an area of previous glacial grounding

Deleted: , streamlined

Deleted: of the bay

Deleted: These elongated features were likely shaped by flowing ice.

Deleted: it is assumed that

Deleted: showed

Deleted: **4.1.1**

located on the eastern end of the surveyed area, close to the modern ice front where a meltwater channel is identified. This feature is about 430 m long, 20 m wide, and 2 m deep.

Potter Cove (Fig. 2c) is separated from Maxwell Bay by a shallow sill, approximately 130 m wide and 12 m high. The seafloor geomorphology in Potter Cove is characterized by numerous transverse features (Fig. 2, A-A'). Although the multibeam survey covers a small portion of the bay (Fig. 2a), transverse ridges across the bay are abundant in the data set. We have classified the transverse ridges into two sets: 1) continuous ridges across the width of the surveyed area, individual ridges symmetrical in cross-section profile, approximately 300-400 m long, 100-160 m wide, and 10-14 m high, and 2) semi-continuous ridges, semi-transverse to the cove, some cross-cutting each other, individual ridges are approximately 50-300 m long, 15-30 m wide, and 1-3 m high, with jagged crests and symmetrical cross-section profiles, located between the larger transverse ridges. Unlike the discrete transverse ridges in the mouth of the bay, ridges proximal to the head of the bay are arcuate and breached by a meltwater channel (280 m long, 8 m wide, and about 1 m deep).

4.2 Hope Bay

The seafloor in inner Hope Bay (Fig. 3) is characterized by several transverse ridges (Fig. 3b, A-A'), while the outer bay is characterized by a large, deep basin (Fig. 3, B-B'). Three sets of transverse ridges are present in the inner bay. Each one of these sets of ridges appears as a composite feature, of more than one ridge stacked on or near one another. The most distal set of transverse ridges is at least 630 m long across inner Hope Bay, approximately 200 m wide, and 15 m high. The next set is 560 m long, with a width of up to 300 m and height ranging 10-20 m. The most proximal set of ridges measure 500 m long, 160 m wide, and 10 m high. The location of the proximal ridges matches the ice extent mapped in the late 1950s (from Cook et al., 2014), which suggests ice was grounded at this site forming the transverse ridges. The seafloor between the proximal set of transverse ridges and the modern ice front is covered by a series of discrete, arcuate-shaped ridges, some cross-cutting each other. The individual ridges are on average 30 m long (but up to 260 m in one case), 10-25 m wide, and 1-3 m high. These features have a symmetrical cross-section profile. Two large promontories separate the inner bay from the outer bay; immediately followed by a large (2 km^2 area) flat-bottomed basin. The outer bay is separated from the Antarctic Sound by a transverse bathymetric high, only partially surveyed, which is cut through by a meltwater channel (50 m deep, 300 m wide) that trends towards the Antarctic Sound (Fig. 3, C-C').

4.3 Lapeyrère Bay

The seafloor in front of Iliad Glacier in Lapeyrère Bay (Fig. 4b) is characterized by poorly-defined, elongated features (Fig.4, E-E') and numerous meltwater channels (Fig. 4, B-B'). The elongated features are symmetrical, approximately 180-300 m long, 40 m wide, and 10 m high. The meltwater channels trend from the ice front margin towards the middle of the inner Lapeyrère Bay, separated from the middle and outer bay by a large transverse ridge (Fig. 4, C-C'). The meltwater

Moved up [2]: Potter Cove (62°13.9'S, 58°41.2'W) (Fig. 4b) is an elongated bay in the southeastern edge of Maxwell Bay. Potter Cove is approximately 4 km long and between 1 km wide in the bay head and 2.5 km wide in the bay mouth. Potter Cove has a small area compared to Maxwell Bay, only approximately 7 km^2, and with water depths ranging between 25-150 m. Fourcade Glacier drains directly into this bay, however most of it terminates on land. The glacier catchment area is about 20 km^2. Ice front retreat of Fourcade Glacier has been approximately 1 km in Potter Cove between 1956 and 2008 (Wolfl et al., 2016), with a greater retreat of grounded ice on the tidewater glacier and much less on the grounded ice on land (Ruckamp et al., 2011).¶

Deleted: Potter Cove¶

Deleted: ¶ ...

Deleted: ¶
4.1.2 Marian Cove¶
Marian Cove (62°12.8'S, 58°46.1'W) (Fig. 4c) is an elongated bay, in the northeastern edge of Maxwell Bay, north of Potter Cove. The bay is approximately 4 km long and between 1-1.5 km wide, with an approximate area of 5 km^2. A single tidewater glacier (with a catchment area of about 15 km^2) drains directly into the bay. It is worth noting that this glacier retreated about 1.7 km between 1956 and 2013 (Lee et al., 2008; Moon et al., 2015). Large meltwater and sediment influx into the bay occur in the summer months (Moon et al., 2015). ¶
¶
Transverse ridges across Marian Cove characterize the seafloor topography. Three major transverse ridges divide the bay into a proximal, middle, and outer basin. The proximal basin has the highest water depths, up to 135 m compared to 120 m and 110 in the middle and outer basin, respectively. The outer, most distal transverse ridge separates Marian Cove from Maxwell Bay. Although this feature is found across the width of the bay, depth varies along the ridge from 40 m in the north to 70 m in the south ...

Moved up [3]: Marian Cove (62°12.8'S, 58°46.1'W) (Fig. 4c) is in the northeastern edge of Maxwell Bay, north of Potter Cove. The bay is approximately 4 km long and between 1-1.5 km wide, with an approximate area of 5 km^2. A single tidewater glacier (with a

Deleted: Trinity Peninsula-

Moved up [4]: Hope Bay (63°24.4'S, 57°2.8'W) (Fig. 5) is located in the northernmost tip of the Antarctic Peninsula, in an area known as Trinity Peninsula, and drains out into the Antarctic Sound. The bay is 6 km long, and between 800 m wide in the bay head and

Deleted: ¶ ...

Formatted: Superscript

Deleted: in addition, a deep channel flows from the inner bay towards the outer bay basin. This basin is flat topped with water depths averaging 320 m. The outer bay is separated from the ...

Deleted: Anvers Island-

Moved up [5]: Lapeyrère Bay (64°25.3'S, 63°17'W) (Fig. 6) is located in northeastern Anvers Island. Lapeyrère Bay is a narrow, elongated bay with water depths varying from 250-740 m, and shallowing towards the fjord walls. The bay is 11 km long, 2 km

Deleted: ¶
¶ ...

channel lengths vary between 1.2 km and 2.5 km, channel widths are up to 200 m, and channel depths are 10-30 m. The transverse ridge is located 2.5 km from the Iliad Glacier front. The ridge is approximately 3 km long and 60 m high; width varies along the ridge, from 500 m near the bay walls to 2500 m in the middle of the inner bay. The ridge has an asymmetrical cross-section profile (Fig. 4, C-C'), with a gentle slope on the proximal side and steeper slope on the distal side. A long (5 km) meltwater channel emerges from the distal side of the transverse ridge and trends towards the middle of the bay (Fig. 4, D-D'). The channel is wide (300 m), with steep walls and a flat base 30 m deep. An elongated ridge is present in the middle bay, parallel to the bay axis. The ridge is about 2.2 km long, up to 400 m wide, and 220 m high. The seafloor in the middle and outer Lapeyrère Bay is smooth and gently dipping towards the outer bay. Abundant slope failures are observed on the steep walls of the fjord. A small, unnamed embayment (5 km long, 2 km wide) is located on northwestern Lapeyrère Bay. An unnamed glacier, with a catchment area of 57 km^2, drains into this unnamed embayment. A sinuous ridge, transverse to ice flow, now breached by meltwater channels and slope failures (Fig. 4, A-A'), is present in the embayment mouth. The transverse ridge has an asymmetrical cross-section profile, it is 2.5 km long, 100 m wide, and up to 70 m high.

4.4 Beascochea Bay

The inner bay area (Fig. 5c), at the convergence of Cadman and Funk glaciers, is separated from the middle bay by an elongated feature, transverse to the bay length. The ridge is about 8 km long, 220 m high, and up 1 km wide. Some areas along this mount are rugged, possibly indicating bedrock. The features present in inner Beascochea Bay are drumlins, glacial lineations, and crag-and-tail landforms. Drumlins are tear-drop shaped, 600-1400 m long, 200-380 m wide, and 20-30 m high. The steep lee side points towards Cadman Glacier and the gentler, stoss side points towards the transverse ridge (Fig. 5, B-B'). CHIRP data shows these are sedimentary features (Fig. 7a). The drumlins are immediately followed by glacial lineations, located at the gentler end of the drumlins. These elongated landforms are 240-2600 m long, 30-170 m wide, and 2-10 m high. Crag-and-tail landforms are located peripherally to the drumlins and lineations, along the bay walls. These elongated features are 200-500m long, 60-120 m wide, and 10-15 m high, and formed by a bedrock knob with a tail of sediment. Middle Beascochea Bay is characterized by a rugged seafloor with linear meltwater channels (Fig. 5, C-C') and large (2.5 km^2), deep (240 m) flat-bottomed basins. The meltwater channels have a V-shaped cross-sectional profile, cut into bedrock and vary in depth (15-60 m), width (80-200 m), and length (200-2000 m). Some of these long, straight channels may be preferentially eroding joints and faults, similar to other areas along the AP shelf (Domack et al., 2006). The bathymetry in outer Beascochea Bay is also rugged, however this region is characterized by an anastomosing network of meltwater channels cutting through bedrock and flowing between elongated mounts, with a few small (<1 km^2 area), deep (50-100 m depth), flat-bottomed basins located between the mounts. Water depths in this area vary between 600-800 m. The meltwater channels vary in depth (20-50 m), width (140-250 m), and length (100-3000 m), some with a V-shaped channel cross-section profiles and others with a U-shaped, flat-bottomed profiles. The channels have abrupt initiation points but terminate,

Deleted: C
Deleted:
Deleted: up to
Deleted: inner bay is separated from the middle bay by a
Deleted: e, interpreted here as a grounding zone wedge,
Deleted: Water depths along the ridge are 280-306 m.
Deleted: s
Deleted: arge
Deleted: , most likely still active,
Deleted: grounding zone wedge
Deleted:
Deleted: flows into
Deleted:
Deleted: linear
Deleted: ; it is 250 m across and
Deleted: in the proximal area, and bifurcates towards the middle of Lapeyrère Bay
Deleted: A streamlined
Deleted: .5
Deleted: ng
Deleted: ,
Deleted: with gentle, lateral slopes, and water depths 340-570 m along the ridge.
Deleted: bay
Deleted:
Deleted: flat
Deleted: , depths up to 740 m,
Deleted: and
Deleted: Several s
Formatted: Superscript
Deleted: ¶
Deleted: ¶ A small, unnamed, embayment (5 km long, 2 km wide) is connected to Lapeyrère Bay in the northwest. Water depths in this area are 2 ...
Deleted: Central Antarctic Peninsula-
Moved up [6]: Beascochea Bay (65°31'S, 63°52.2'W) (Fig. 7) is
Deleted: ¶
Deleted: 7c
Deleted: d mount
Deleted:
Formatted: Superscript

generally, into the small basins that connect to other channels. Channel orientations vary from parallel to oblique to bay axis. The elongated mounts are asymmetric, carved in bedrock, with varying length (260-5000 m), width (210-1000 m), and height (15-90 m).

Lever Glacier cove is separated from middle Beascochea Bay by a transverse ridge (Fig. 5, D-D'). This feature has been partially surveyed but shows a wedge-shaped cross-sectional profile, steep distal side and gentler proximal side. The ridge is at least 5 km long, up to 1.5 km wide, and a height between 70 and 180 m. Another transverse ridge is located less than 1 km from the modern ice front of Lever Glacier. The ridge was only surveyed in the northern area of the cove but it is likely present across the bay, next to the modern glacier front. It is sinuous (about 2.5 km long, 20 m high) with a prominent knob in the middle of the cove. This knob coincides with the deepest area in the cove, enhancing it further in the bathymetry. The seafloor of this cove is covered by glacial lineations (Fig. 5, A-A') present from the proximal to the distal transverse ridges. The lineations are semi-parallel to the axis of the cove, individual features have a symmetric cross-sectional profile, and vary in length (400-1400 m), width (100-150 m), and heights (5-10 m), as well as the distance between the ridge crests (90-260 m). Although water depths within the cove vary from 120-320 m, the glacial lineations are present throughout the cove regardless of water depth (Fig. 5b). In the CHIRP dataset, the lineations are characterized by a strong surface with no internal reflectors, which likely indicates till (Fig. 7).

Funk Glacier cove and inner Beascochea Bay are separated by a large (2.3 km long, 800-1000 m wide, 60-150 high), wedge-shaped transverse ridge (Fig. 5, E-E'). The eastern (proximal) side of the ridge is covered by a 20-m high, 1.4-km long feature that resembles a mass wasting deposit. However, this feature could also be the result of meltwater deposition generated when the ice was grounded nearby. Higher resolution multibeam data are needed to better characterize this feature and sediment analysis to interpret its depositional origin. Several glacial lineations are present on the seafloor and can be traced from the middle of the cove to the modern front of Funk Glacier. Individual features have a symmetrical cross-sectional profile, are parallel to one another, and have varying height (5-20 m), width (40-100 m), and length (160-700 m). Unlike the lineations in Lever Glacier cove, the subsurface of these landforms resembles an amalgamation or stacked sediment packages (Fig. 7b), most likely recently reworked till. A network of meltwater channels originate near the ice front and trend towards the middle of the fjord. Channel depths vary (6-20 m), as well as widths (30-200 m), and lengths (70-1200 m).

In Cadman Glacier cove we identify large promontories (up to 300 m high) on each side of the cove mouth, separating the cove from inner Beascochea Bay (Fig. 5c). Abundant slope failures are present on the sides of the promontories. The middle of the cove has a flat basin with water depths down to 550 m.

Deleted: The depths along this feature vary between 270-370 m, and shallowing towards the fjord walls. This elongated feature in likely a grounding zone wedge. Two major submarine landforms are present in the seafloor of inner Beascochea Bay, drumlins and flutings, in an otherwise flat basin. The drumlins are tear-drop shaped, length and width varies between 350-1200 m and 120-400 m, respectively. The drumlins have a steep end that points towards Cadman Glacier and a gentler end that points towards the bay mount in the inner bay. The steep ends of the drumlins are between 10-40 m high. The CHIRP shows these features are covered by a thin sediment layer. The drumlins are immediately followed by flutings, located at the gentler end of the drumlins. These flutings are very subtle features on the seafloor, 8-10 m high and 500-1000 m long. Another set of flutings occurs on the sides of the inner bay basin, along the bay walls. These flutings are parallel to the drumlins and to the first set of flutings. However, the flutings on the basin walls are much shorter in average, 300-400 m long. We hypothesize the differences in size and length are explained by differences in the material forming the elongated feature (till vs. bedrock), or the amount of deformable material available in the area (channel vs. bay walls). Another reason may be the strength exerted by the ice molding these sediments; the bottom of the glacier would easily mold sediments or till for a longer period of time, while the glacier margins would not exert the same force along the bay walls and therefore the resulting features would be shorter. ¶
¶
The middle of Beascochea Bay is characterized by a rugged seafloor and only two different features are distinguished, channels and a large basin. The channels vary in depth (15-60 m), width (80-200 m), length (200-2000 m), and overall, the channels are linear, cut ...

Deleted: 4.4.1 Lever Glacier Cove¶

Moved up [7]: (65°30.7'S, 63°43.4'W) (Fig. 7b) An elongated bay, 6 km long and 3 km wide, with a bay area of about 16 km^2. The largest glacier draining into this cove is Lever Glacier (catchment

Deleted: A grounding zone wedge…ransverse ridge separates t ...

Moved (insertion) [10]

Deleted: grounding zone wedge was only surveyed in the north ...

Moved up [10]: The grounding zone wedge was only surveyed in the northern area of the cove but it is likely present across the bay.

Deleted: The grounding zone wedge was only surveyed in the northern area of the cove but it is likely present across the bay ...

Deleted: 4.4.2 Funk Glacier Cove¶

Moved up [8]: (65°34.8'S, 63°45.4'W) (Fig. 7c) An elongated bay, 4 km long and 2 km wide, with a bay area of about 8 km^2. A large glacier drains directly into this cove, Funk Glacier, with a

Deleted: A large (2.3 km long, 800-1000 m wide, 60-150 high) ...

Deleted: ¶
4.4.3 Cadman Glacier Cove¶

Formatted: Font: Not Bold

Moved up [9]: (65°36.7'S, 63°48.7'W) (Fig. 7c) This cove is the smallest in Beascochea Bay, it is 3 km long and 3 km wide, the bay

Deleted: The area surveyed in the cove is insufficient to map large seafloor features, if there are any present in the seafloor. Nevertheless, we…identify two…large promontories (up to 300 m ...

5 Discussion

5.1 Distribution and interpretation of seafloor features

We have described numerous seafloor features in four bays in the western AP (additional bays are shown in the supplementary material). Many of the bays show similar landform distributions and therefore we propose a schematic model representative of an assemblage of submarine landforms in bays from the western AP (Fig. 8). This spatial distribution of landforms, from the modern ice front to the outer bay area, results from combining the geomorphology of all the bays presented. The inner bay is characterized by glacial lineations, straight meltwater channels, and in some cases moraines and crevasse squeeze ridges. The inner bay and middle bay are typically separated by a transverse ridge. The middle bay is characterized by deep, flat-bottomed basins and, in some examples, drumlinoid features (drumlins and/or crag-and-tails), with the stoss end pointing towards the outer bay. In most cases, the middle and outer bay are separated by another, likely larger, transverse ridge, which is immediately followed by large, asymmetrical, streamlined (elongated) features and meltwater channels in the outer bay. Although some seafloor features are common, we recognize there is some variation between the bays and within the bays themselves (Fig. 9).

Models showing geomorphic features have been presented largely for the continental shelf in Antarctica (Wellner et al., 2001; Canals et al., 2002; Evans et al., 2004; Dowdeswell et al., 2008; Graham et al., 2009), and therefore our model differs from them since we show landforms focused in the confined bay areas. Our proposed schematic model is similar to other models of landform assemblages presented for glaciated environments in Svalbard (Ottesen and Dowdeswell, 2009) and Greenland (Dowdeswell et al., 2016). However, unlike the Ottesen and Dowdeswell (2009) model for restricted areas like fjords where the seafloor is dominated by landforms transverse to ice flow, our findings in AP fjords show a combination of landforms parallel and transverse to ice flow (Fig. 8). In addition, AP fjords show evidence of subglacial meltwater flow in the form of channels carved in bedrock. Figure 9 shows the distribution of submarine landforms per bay compared to the area of the bay and the combined catchment area of the glaciers draining into each bay (also shown in supplementary material tables). These features were likely formed during the final ice retreat phase throughout the AP bays during the Last Glacial Maximum. However, features carved in bedrock (e.g. meltwater channels, streamlined features) are likely the result of multiple cycles of glaciation in the bays, similar to other areas on the Antarctic continental shelf (Ó Cofaigh et al., 2005; Anderson and Fretwell, 2008; Graham et al., 2009; Livingstone et al., 2013). The submarine landforms are classified into three categories based on their depositional environment and sedimentary processes forming them: 1) subglacial landforms, 2) ice-marginal landforms, and 3) recent sediment reworking throughout the bays.

5.1.1 Subglacial landforms

Elongated, parallel ridges: glacial lineations

Deleted: ¶
5

Deleted: 8

Deleted: continuum of landform features

Deleted: flutings

Deleted: and linear

Deleted: The

Deleted: a grounding zone wedge

Deleted: topped

Deleted: cases

Deleted: drumlins

Deleted: ir

Deleted: hallow

Deleted: T

Deleted: grounding zone wedge

Deleted:

Deleted: Meltwater channels and smaller, flat-topped basins are common in the outer bay.

Deleted: o

Deleted: The main difference is that our model shows more details within the bays and we do not extend our study to the continental shelf as the models from the northern hemisphere. In addition, unlike the bays in those models, we show that some AP bays include: 1) multiple transverse features, ex. GZW and moraines, 2) meltwater channels throughout the bays, and 3) a transition zone between bedrock and sediment substrate, which results in the formation of different seafloor landforms.

Deleted: 9

Deleted: actual

Moved (insertion) [11]

Deleted: by ice advancing (and later retreating)

Deleted:

Deleted: and out into the continental shelf

Moved up [11]: These features were likely formed by ice advancing (and later retreating) throughout the bays and out into the continental shelf during the Last Glacial Maximum.

Deleted: However, features carved in bedrock (e.g. meltwater channels, streamlined features) are likely the result of multiple glaciation cycles in the bays, similar to other areas in the Antarctic continental shelf (Ó Cofaigh et al., 2005; Anderson and Fretwell, 2008; Graham et al., 2009; Livingstone et al., 2013). Drumlins, GZW, moraines and basins appear in lower numbers in the bays, ...

Deleted: four

Deleted: landforms formed by glacial retreat and minor re-adva ...

Deleted: ¶

Formatted: Font: Bold

Elongated ridges parallel to bay axis are interpreted as glacial lineations (Fig. 6a). In this study, lineations vary in length (between 80 m and 2.7 km long), width (between 5 and 200 m), and height (between 1 and 20 m high). Glacial lineations typically occur in groups in the inner bay (Fig. 2b, 4b, 5b-c), while in some cases lineations are also present in the middle bay area (Supplementary material Fig. 1). Glacial lineations form under flowing ice over a thin deformation till layer; most glacial lineation heights in this study are less than 10 m. The lineations are parallel to the former ice flow direction. In CHIRP, some lineations have a strong surface with no internal reflectors, while others are formed by stacked sediment packages of reworked sediment (Fig. 7).

Teardrop-shaped ridges in sediment: drumlins

Streamlined, teardrop-shaped ridges formed in deformable sediment are interpreted as drumlins (Fig. 6c). The stoss side indicates ice flow direction towards the bay mouth. Drumlins are covered by parallel acoustically laminated sediment (Fig. 7a). These features are observed in Beascochea Bay (Fig. 5d) and Andvord Bay (Supplementary material Figs. 1, 4), both very large bays (Fig. 9). In both examples, the drumlins occur in an area of ice flow convergence from two large drainage systems. This convergence may result in flow acceleration, which would explain the formation of the drumlins (Wellner et al., 2001; 2006; Larter et al., 2009).

Teardrop-shaped ridges in bedrock: crag-and-tails

Streamlined, teardrop ridges formed in bedrock with a sediment tail are interpreted as crag-and-tails (Fig. 6d). These features are present in Beascochea Bay (Fig. 5d) and Andvord Bay (Supplementary material Figs. 1, 4), where they are associated with drumlins and glacial lineations. Crag-and-tail features are also present in Brialmont Cove, Flandres Bay, and Collins Bay, all broad bays (Fig. 9). These features vary in length (130-900 m), width (40-300 m), and height (2-28 m), but are in general smaller than drumlins and shorter than glacial lineations. Crag-and -tails are parallel to ice flow direction in the bays.

Elongated, asymmetrical ridges in bedrock: streamlined features

Large, elongated streamlined features are found in the outer bays carved in bedrock (Fig. 6b), as shown by the bowtie or hummocky reflections in the CHIRP data (Fig. 7). Actively flowing ice carved them in bedrock, most likely over multiple glaciation events (Anderson and Fretwell, 2008; Graham et al., 2009; Livingstone et al., 2013). These features are typically not symmetrical and in some areas are more elongated closer to the bay mouth and become stubbier away from the bay (Fig. 5d). Elongation at the bay mouth may indicate faster ice flow at those locations and then later deceleration as the ice reaches a larger, open area to flow outside of the confined bay (Bradwell et al., 2008).

Subglacial meltwater channels

Subglacial meltwater channels (Fig. 6d) have been carved into crystalline bedrock, in the inner bay areas (Fig. 4b) and in the outer bay areas (Fig. 5b, c). In addition, channels are more frequent in the southern bays. The meltwater channels mapped in

Formatted: Font: Bold

Formatted: Font: Bold

Formatted: Font: Bold

Deleted: The flutings are interpreted to be formed by flowing ice over a thin deformation till layer; most fluting thicknesses are less than 10 m. Flutes are usually parallel to the ice flow direction, and usually form as ice flow encounters an obstacle, large rock or bedrock, in the up-ice end and subglacial sediment flows to the back of the obstacle, forming an elongated ridge in the lee side (Bennett and Glasser, 2009).

Formatted: Font: Bold

Formatted: Font: Bold

Formatted: Font: Bold

Formatted: Font: Bold

Formatted: Font: Bold

Moved (insertion) [12]

Deleted: The streamlined features are

Deleted: ,

Deleted: where a

Deleted: .

Formatted: Font: Bold

Moved (insertion) [13]

Deleted: mostly

Deleted: the number of channels increases this study area indicate a complex network of flow, with short straight and anastomosing channels. Similar meltwater channels have been mapped in other Antarctic regions with crystalline bedrock (Lowe and Anderson, 2002; Anderson and Fretwell, 2008; Livingstone et al., 2013; Nitsche et al., 2013), and likely also formed through multiple glaciation events. The presence of these channels highlights the production of subglacial meltwater in the northern AP region, previously only identified in southern AP areas (Dowdeswell et al., 2004; Anderson and Fretwell, 2008; Livingstone et al., 2013).

Basin fill from subglacial sediment deposition

Several meltwater channels are associated with small flat-bottomed basins (Fig. 5d, 6d), similar to those found in other areas in the Antarctic continental shelf, interpreted as palaeo-subglacial lakes (Kuhn et al., 2017). Flat-bottomed basins have acoustically parallel sediment fill (Fig. 7). Subglacial sediment deposition occurs through subglacial meltwater flow and through tidal pumping, close to the grounding line (Domack, 1990; Domack et al., 2006).

5.1.2 Ice-marginal landforms

Large transverse ridges: grounding zone wedges

Large, transverse sedimentary ridges, usually formed at narrow locations in the bay perimeter are interpreted as grounding zone wedges (GZW) (Fig. 6e). These landforms are characterized by a strong surface with no internal reflectors (Fig. 7). GZW are depositional features, formed during stillstand periods during a general ice retreat, when sediment is carried to the grounding line through bed deformation and basal melting (Alley et al., 1989; Anderson, 1999; Dowdeswell et al., 2008; Batchelor and Dowdeswell, 2015). Most of the GZW observed in the western AP bays are asymmetric, with a steep slope distal and gentler slope proximal to the ice front (Figs. 4, 5). The geometry of these transverse ridges is similar to much larger GZW in the Ross Sea (Halberstadt et al., 2016) and the Weddell Sea (Campo et al., 2017). The size of the GZW has been correlated with the length of ice stability (Alley et al., 2007; Dowdeswell and Vasquez, 2013; Batchelor and Dowdeswell., 2015), a larger GZW imply a longer period of ice stability.

Small transverse ridges: moraines

Moraines are small sedimentary ridges that can be transverse to the bay axis or arcuate, forming a lunate shape across the bay (Figs. 6g, 2, 3). These transverse ridges can form through various processes including melting out of basal and englacial debris-rich ice, ice push, dumping of supraglacial debris, and lodgement (Powell, 1981; Powell and Domack, 1995; Batchelor and Dowdeswell, 2015). The moraines are interpreted to form during ice retreat, but unlike the GZW, the duration of the stillstand is much shorter, and possibly more frequent (Ottesen et al., 2005; Batchelor and Dowdeswell, 2015).

Small ridges in networks: crevasse squeeze ridges

Small ridges, cross cutting each other, forming a network are interpreted as crevasse squeeze ridges (Figs. 6g). These only occur in two bays (Fig. 2, 3), in proximal settings with shallow water depths (<120 m). Crevasse squeeze ridges are not a

Deleted: form

Deleted: channels

Moved (insertion) [16]

Deleted: A complex network of channels carved in bedrock, interpreted as subglacial meltwater channels, that

Formatted: Font: Bold

Formatted: Font: Bold

Moved up [12]: The streamlined features are found in the outer bays, where actively flowing ice carved them in bedrock, most likely over multiple glaciation events (Anderson and Fretwell, 2008; Graham et al., 2009; Livingstone et al., 2013). These features are not symmetrical and in some areas are more elongated closer to the bay mouth and become stubbier away from the bay. Elongation at the bay mouth may indicate faster ice flow at those locations and then later deceleration as the ice reaches a larger, open area to flow outside of the confined bay (Bradwell et al., 2008). Subglacial meltwater channels have been carved into crystalline bedrock, mostly in the outer bay areas. In addition, the number of channels increases in the southern bays. The meltwater channels mapped in this study area form a complex network of flow, with short straight channels and anastomosing channels. Similar meltwater channels have been mapped in other Antarctic regions with crystalline bedrock (Lowe and Anderson, 2002; Anderson and Fretwell, 2008; Livingstone et al., 2013; Nitsche et al., 2013), and likely also formed through multiple glaciation events. The flutings are interpreted to be formed by flowing ice over a thin deformation till layer; most fluting thicknesses are less than 10 m. Flutes are usually parallel to the ice flow direction, and usually form as ice flow encounters an obstacle, large rock or bedrock, in the up-ice end and subglacial sediment flows to the back of the obstacle, forming an elongated ridge in the lee side (Bennett and Glasser, 2009). Drumlins are observed in the middle of bays, recording ice flow direction towards the bay mouth. They are covered by parallel laminated sediment (Fig. 3) and have been interpreted as forming at the transition between crystalline bedrock and sedimentary strata marking the onset of accelerating flow (Wellner et al., 2001, 2006). This acceleration may be the result of converging flow from different directions in Anvord Bay and Beascochea Bay. ¶
¶

Moved up [13]: Subglacial meltwater channels have been carved into crystalline bedrock, mostly in the outer bay areas. In addition, the number of channels increases in the southern bays. The meltwater channels mapped in this study area form a complex network of flow, with short straight channels and anastomosing channels. Similar meltwater channels have been mapped in other Antarctic regions with crystalline bedrock (Lowe and Anderson, 2002; Anderson and Fretwell, 2008; Livingstone et al., 2013; Nitsche et al., 2013), and likely also formed through multiple glaciation events.

Deleted: Subglacial landforms include streamlined features, meltwater channels, flutings (mapped in the middle of bays) and drumlins (Fig. 2). The streamlined features are found in the outer bays, where actively flowing ice carved them in bedrock, most lik ...

Formatted: Font: Bold

Formatted: Font: Bold

Moved (insertion) [14]

common feature in Antarctica, however they have been observed in the Amundsen Sea embayment (Klages et al., 2013). These landforms have been reported in Iceland (Bennett and Glasser, 2009) and Svalbard (Ottesen and Dowdeswell, 2006, 2009) occurring either as symmetrical, low ridges, or as rhombohedral ridges, about 5 m high, found on the ice proximal margin of moraines. These ridges form by squeezing till in crevasses formed at the base of grounded ice, and they indicate ice stagnation followed by a rapid uncoupling from the seafloor (Powell and Domack, 1995; Ottesen and Dowdeswell, 2006; Bennett and Glasser, 2009). The preservation of these features indicates that no further ice front re-advance has occurred over them.

5.1.3 Recent sediment reworking throughout the bays

Slope failures: mass wasting and gullies

Slope failures occur in transverse ridges (either moraines or GZW) that result in the formation of a large fan-shaped feature in the bays (Figs. 2, 5). These features are not common in these bays but they are observed in the inner bay areas. Lobes are between 200-1200 m long and 300-500 m wide. The characteristic steep walls of the glacial valleys have gullies (Fig. 6f) throughout the perimeter of the bays, although in some bays gullies are more abundant than in others (Figs. 9, 10).

Proglacial meltwater channels

Straight, long, wide channels, carved in soft sediment, are interpreted as a modern erosional feature (Fig. 4b). These channels are differentiated from the subglacial meltwater channels by their linear channel axis, although some are slightly sinuous, they do not form complex flow networks, some are observed in low numbers or even isolated in a bay (Fig. 4b). These types of channels are common in Chilean bays (Dowdeswell and Vasquez, 2013) and northern hemisphere fjords (Syvitski et al., 1987; Bennett and Glasser, 2009) where they form by dense sediment flows or turbidity currents resulting from glacifluvial meltwater or slope failures (Syvitsky et al., 1987; Dowdeswell and Vasquez, 2013).

Basin fill from turbid meltwater and rainout

The proglacial channels carry sediment flows from bathymetric high regions to deep basins (Fig. 6 b, d, f), where sediment of varying sizes is deposited in layers, forming the acoustically laminated basin fill (Fig. 7). In addition, hemipelagic processes (Powell and Domack, 1995; Ó Cofaigh and Dowdeswell, 2001; Domack et al., 2006) and meltwater plumes originating at the glacier terminus (Domack et al., 1994; Domack et al., 2006) contribute to sediment deposition in basins. Sediment reworking processes have likely been occurring since grounded ice started retreating, however, the recent warming period in the AP area may have contributed to an increase in meltwater production which may have resulted in larger sediment reworking.

5.2 Observations on ice flow dynamics

Deleted: In the bays observed in this study, crevasse squeeze ridges were found proximal to the ice front and in water depths shallower than 120 m.

Deleted: ¶
The grounding zone wedges (GZW) are classified as ice marginal landforms. The GZW are large, transverse sedimentary ridges, usually formed at narrow locations in the bay perimeter. GZW are interpreted as depositional features, formed during stillstands periods during a general ice retreat, when sediment is carried to the grounding line through bed deformation and basal melting (Alley et al., 1989; Anderson, 1999; Dowdeswell et al., 2008; Batchelor and Dowdeswell, 2015). Most of the GZW observed in the western AP bays are asymmetric, with a steep slope distal and gentler slope proximal to the ice front. The geometry of these transverse ridges is similar to much larger GZW in the Ross Sea (Halberstadt et al., 2016) and the Weddell Sea (Campo et al., 2017). The size of the GZW has been correlated with the length of ice stability (Alley et al., 2007; Dowdeswell and Vasquez, 2013; Batchelor and Dowdeswell., 2015), a GZW with a large volume implies a period of longer ice stability. In addition, if the amount of sediment flux is known, then we could estimate the duration of ice grounding at that location (Howat and Domack, 2003). ¶
¶
5.1.3 Landforms formed by glacial retreat and minor ice re-advance events¶
Features formed during glacial retreat and minor re-advance events include moraines, flutings (mapped close to the modern ice front), and crevasse squeeze ridges. Moraines are small sedimentary ridges that can be transverse to the bay length or arcuate, forming a lunate shape across the bay length. The moraines are interpreted to form during ice retreat, but unlike the GZW, the duration of the stillstand is much shorter, and possibly more frequent (Ottesen et al., 2005; Batchelor and Dowdeswell, 2015). The moraines likely formed as ice pushed sediment during a minor readvance, in a general retreat phase (Ottesen and Dowdeswell, 2006; Batchelor and Dowdeswe ...

Moved up [14]: Crevasse squeeze ridges are not a common feature in Antarctica, however they have been observed in the Amundsen Sea embayment (Klages et al., 2013). These landforms

Deleted: ¶
¶

Deleted: 4

Formatted: Font: Not Bold

Formatted: Font: Bold

Formatted: Font: Bold

Moved (insertion) [15]

Deleted: Two different types of channels were identified in this study: 1) linear

Deleted: .

Formatted: Font: Not Bold

Formatted: Font: Bold

Deleted: ¶
Features formed by recent sediment reworking include slope failures, linear channels, and deep basin fill. The characteristic ste ...

Formatted: Font: Not Bold

There is a variable spatial distribution of the submarine landforms presented in this study (Fig. 1). Although, we present a generic model representative of the geomorphology in the western AP bays (Fig. 8), it is clear that not all the features are present in all the bays and therefore we examined the local conditions in order to understand ice flow in the western AP.

5.2.1 Latitude and temperature gradient

Although there are some latitudinal differences between the bays observed, Marian Cove (62°12'S) at the north, and Cadman Glacier cove (65°36'S) at the south, we did not find a direct correlation between latitude and the number of features found in the bays (Fig. 11a). However, the number of glacial lineations and meltwater channels increased towards the southern AP (Figs. 9 and 10). In addition, the complexity of the meltwater channel flow networks increased towards the south AP.

In northern locations in our study area, the seafloor has a lower relief, e.g. Maxwell Bay (Fig. 2) and Hope Bay (Fig. 3). Although there are some bathymetric highs, the seafloor appears smoother overall. In comparison, the southern bays have a more rugged seafloor, with very high differences in relief, e.g. Flandres Bay (supplementary material Fig. 6) and Beascochea Bay (Fig. 5). The deep basins with flat bottoms in Flandres Bay and Beascochea Bay contrast with the variable relief around them. We attribute these differences in seafloor roughness to a higher sediment cover in the northern areas compared to the southern areas. The increased sediment cover is related to higher sediment accumulation rates, documented in Maxwell Bay by Milliken et al. (2009) and Boldt et al. (2013). Thus the smooth seafloor is likely due to burial of glacial features. The smooth seafloor cover in Maxwell Bay has more resemblance with Chilean fjords (e.g. Dowdeswell and Vasquez, 2013) and bays in South Georgia (e.g. Hodgson et al., 2014) than it does with other AP bays.

5.2.2 Bay area and glacier drainage area

One of the apparent variables in this comparison is the size of the bay area and the catchment area of the glaciers draining into any particular bay (Fig. 9). A reasonable assumption is that a larger drainage area would likely result in larger amounts of sediment and meltwater delivered to the seafloor, which could potentially form more seafloor features as ice flows in the bay. We compared bay area and glacier catchment area (total combined area of the glaciers draining into each bay) to the number of features mapped in the bays. We found a relatively high correlation between the bay area and the number of features (Fig. 11e), and a very poor correlation with total glacier catchment area (Fig. 11f). Larger bays have, in average, more submarine landforms, but a larger drainage area does not result in more submarine landforms in the bay. This conclusion implies that landform formation is complex and not directly dependent on the amount of ice flow into the bays.

When comparing glacier catchment areas to the type of features found (Fig. 9), the smaller drainage areas are correlated with the smaller size features, e.g. moraines, which are not found in bays with larger catchment drainage areas. This suggests that smaller fluctuations in the ice flow (that would result in the formation of smaller landforms) would not be apparent in larger glacial systems. Therefore, we conclude that the size of the bays, and not the size of the catchment area, dictates the number

Deleted: 8

Deleted: C

Deleted: 11a

Deleted: flutings

Deleted: 9

Deleted: 10

Deleted: This is consistent with the higher latitudinal locations of meltwater channels identified in other studies (Lowe and Anderson, 2002; Anderson and Fretwell, 2008; Livingstone et al., 2013; Nitsche et al., 2013).¶

Deleted: bay

Deleted: 4

Deleted: 5

Deleted: 5

Deleted: 7

Deleted: tops

Deleted: , and not necessarily to differences in bedrock topography

Deleted: lack of geomorphic features on the modern

Deleted:

Deleted: cannot be interpreted to indicate lack of their formation

Deleted: In fact, t

Deleted: 9

Deleted: In addition, a larger bay would likely have a larger number of landforms.

Deleted: 11e

Deleted: 11f

Deleted: 9

Deleted: ex.

Deleted: and crevasse squeeze ridges of features that form in the seafloor, but smaller glacier catchment areas are able to preserve evidence of small fluctuations in ice flow. This conclusion is consistent with results from Bourgeois Fjord and Blind Bay (Garcia et al., 2016), near Marguerite Bay in the southern AP, where an inverse relation between drainage basin size and retreat of the glacier terminus was found. Similarly, Fox and Cooper (1998) measured the largest size reduction on the smaller ice bodies in the AP.

5.2.3 Geometry of bays

Since there is a large degree of variability regarding size of the bays (Fig. 9), we additionally analysed the bay length, bay width, and bay ratio (length/width). Bays with ratios lower than 1 were classified as open bays, ratios between 1 and 2 were classified as broad bays, and ratios higher than 2 were classified as narrow bays. We refer to this classification as the geometry of the bays. This geometry was compared to the type (and number) of features found in each observed bay (Fig. 10b). Because most bays in our study area were classified as narrow, we use "percentage of bays" as a way to normalize the results. Therefore, we refer to the percentage of narrow (or combined broad and open) bays where certain feature was identified; for example, Fig. 10(b) shows that 78% of the narrow bays have GZW, while only 28% of the broad/open bays have this same type of feature.

In Fig. 10(b) we note that crevasse squeeze ridges, moraines and drumlins occur only in narrow bays; GZW and glacial lineations occur mostly in narrow bays; crag-and-tails occur mostly in broad/open bays; and streamlined features, gullies/slope failures, meltwater channels, and basins tend occur all bays regardless of the bay geometry. In addition, we compared bay length, bay width, and bay ratio to the number of features mapped (Fig. 11 b-d). We see that both, bay length and width, have a high correlation with the number of features found in the bay.

From these observations, we conclude that the geometry of the bay dictates the types of features that form. Narrower bays tend to form transverse features, like moraines and GZW, which form during periods of ice stabilization (Anderson, 1999; Alley et al., 2007; Dowdeswell et al., 2008; Dowdeswell and Vasquez, 2013; Batchelor and Dowdeswell., 2015). The width of the glacial valley has been suggested to play an important role for glacial flow (O'Neel et al., 2005; Joughin et al., 2008; Robel et al., 2017). Similarly, widths of ice-stream troughs, along with water depth, control ice flow by increasing the lateral resistance (Whillans and van deer Veen, 1997; Jamieson et al., 2012). Lateral drag increases as the width narrows which may lead to ice stabilization that could result in transverse features, based on the amount of sediment flux and duration of the still-stand (Howat and Domack, 2003; Dowdeswell and Vasquez, 2013). Transverse-to-flow features in the Ross Sea and Weddell Sea (Halberstadt et al., 2016; Campo et al., 2017) are larger than the GZW and moraines identified in this study and are the result of a much larger ice flow system. Therefore, width may play a major role in confined flow, e.g. fjords and bays.

5.3 Comparison to other glaciated regions

Deleted: record

Deleted: 9

Deleted: 10

Deleted: and Table 1 in supplementary material).

Deleted: 10

Deleted: 100

Deleted: 42

Deleted: 10

Deleted: , and moraines

Deleted: and

Deleted: mostly in broad/open bays. Basins and flutings tend to occur in

Deleted: , and no feature type occurs exclusively in open bays.

Deleted: 11

Deleted: strong

Deleted: , while bay ratio does not show any correlation.

Deleted: observations

Deleted: bay length and bay width exert a large control over the number of features found, and that

Deleted: The l

Deleted: 5.2.4 Seafloor lithology¶
The CHIRP dataset was used to identify the lithology and sediment thicknesses of some of the features mapped in the bays (Fig. 3). Five facies were identified throughout the study area and two localized examples (drumlins and flutings) because they present a unique internal acoustic configuration. The GZW and moraines are characterized by a strong surface with no internal reflectors; basins have thinly laminated sediments; the streamlined features and the meltwater channels were both carved in bedrock and they form bowtie or hummocky reflections; drumlins have a thin sediment cover; and flutings show either a hard surface and no internal reflectors or they show thick, amalgamated packages of reworked sediment.¶
¶
Two different types of channels were identified in this study: 1) linear, wide channels, carved in soft sediment, interpreted as a modern erosional feature. These types of channels are common in Chilean bays (Dowdeswell and Vasquez, 2013) and northern hemisphere fjords (Syvitski et al., 1987; Bennett and Glasser, 2009) where they form by dense sediment flows or turbidity currents resulting from glacifluvial meltwater or slope failures. And 2) A complex network of channels carved in bedrock, interpreted as subglacial meltwater channels, that highlight the production of subglacial meltwater in the northern AP region, previously only identified in southern AP areas (Dowdeswell et al., 2004; Anderson and Fretwell, 2008; Livingstone et al., 2013). ¶
¶ ...

Moved up [15]: Two different types of channels were identified linear, wide channels, carved in soft sediment, interpreted as a

Moved up [16]: A complex network of channels carved in bedrock, interpreted as subglacial meltwater channels, that highlight

Similar assemblages of submarine landforms are found in bays of Greenland (Dowdeswell et al., 2016) and, to a lesser extent, in Svalbard (Ottesen and Dowdeswell, 2009). In Greenland, Dowdeswell et al. (2016) observed lineations near the modern ice front followed by a Little Ice Age moraine with channels flowing towards a deep basin in the middle of the fjord, and streamlined features in the outer fjord areas. In Svalbard, several transverse retreat moraines and a larger Little Ice Age moraine ridge characterize the inner bay, followed by drumlinoid features in the middle to outer bay and larger transverse ridges in the outer fjord (Ottesen and Dowdeswell, 2009). Because Svalbard experiences higher sedimentation rates, compared to the AP, it is possible that some of the features seemingly not present may actually be covered.

Bays in South Georgia, an island northeast of the AP, also show some similarities to west AP bays; a shallower inner bay, followed by a moraine and a deep basin towards the outer bay (Hodgson et al., 2014). However, many of the bays in South Georgia have smooth seafloors, which indicates any other older features (if any) are likely buried. Dowdeswell and Vasquez (2013) mapped the geomorphology of some bays near the Southern Patagonian Ice Cap in Chile, and they show less similarities to western AP bays in general. Bays in Chile are dominated by meltwater production that is reworking and redistributing the sediment, draping the seafloor, creating a smooth cover throughout (Dowdeswell and Vasquez, 2013). Much less meltwater production and sediment reworking, along with relatively less sediment cover in the western AP bays, has enabled us to map submarine landforms in detail.

5.4 Possible late Holocene glacial advance

The seafloor in the ice proximal area in several of the bays presented in this study is characterized by a proximal transverse ridge, in most cases with glacial lineations, located a few kilometres from the modern ice front; Marian Cove (Fig. 12b), Hope Bay (Fig. 12c), Lapeyrère Bay (Fig. 12d), Fournier Bay (Fig. 12e), Moser Glacier Cove (Fig. 12f), Briand Fjord (Fig. 12g), Lever Glacier cove (Fig. 12h), and Funk Glacier cove (Fig. 12i) show these features. We propose these proximal features are associated with a Little Ice Age (LIA) glacial advance. Similar sets of features (an ice proximal transverse ridge followed by either smaller transverse ridges or elongated ridges parallel to the modern ice front) in the inner bays have also been observed in Chile (Dowdeswell and Vasquez, 2013), Greenland (Dowdeswell et al., 2016), and Svalbard (Ottesen et al., 2005; Ottesen and Dowdeswell, 2009) and have been interpreted as LIA landforms. In Antarctica, there has been less published research associating geomorphology and the LIA. Christ et al. (2014) observed these same set of features in the ice proximal region of Barilari Bay (Fig. 12j) and referred to them as a "fluted grounding zone wedge". They suggest a cooling and glacial advance between 1220 and 1868 A.D. (Christ et al., 2014) based on sedimentological analysis and ^{210}Pb and radiocarbon dates. Garcia et al. (2016) describe the geomorphology of a western AP fjord near Marguerite Bay, south of our study area. They show transverse, crescent-shape, and longitudinal ridges ("morainic" landforms), along with elongated ridges, semi parallel to the fjord length in the inner bay. Although they do not present any sedimentological analysis or dating, they interpret these inner features as a result of LIA glacial advance in this fjord because these submarine landforms appear pristine, with no evidence of a subsequent glacier advance, relatively recent, and are located only a few kilometres

Deleted: allows

Deleted: The presence of meltwater channels in the middle to outer bays, carving into bedrock, is an important characteristic that is only present in AP bays and not in the other regions mentioned above.

Deleted: L

Deleted: (

Deleted: ster

Deleted: C

Deleted: C

Deleted: is characterized by a grounding zone wedge (GZW) located a few kilometres from the modern ice front with flutings between the GZW and the modern ice front (Fig. 12).

Deleted: a large,

Deleted: much less

Deleted: has been published

Deleted: also

Deleted: 12j

Deleted: Although, they do not interpret the submarine landforms or the possible formation mechanisms, they do argue for LIA formation

Deleted:

from the modern ice front. In Potter Cove (Fig. 2c), transverse moraines in the inner cove are likely associated with LIA advance (Wolfl et al., 2016), however no dating was conducted on those features. In the neighbouring Maxwell Bay (Fig. 2), no sedimentological evidence was found of LIA advance (Milliken et al., 2009), which may indicate that if there was any LIA advance in the western AP bays, only smaller systems (narrow bays) and/or shallow bays would record and preserve any geomorphic evidence, as suggested by our observations above. The LIA event has been reported in western AP bays and the South Shetland Island by several authors (Domack et al., 1995; Shevenell et al., 1996; Domack et al., 2001; Domack et al., 2003; Hall, 2007; Hass et al., 2010; Monien et al., 2011; Simms et al., 2012) but it may be a more widespread event throughout the AP than previously assumed. However, it is worth noting that LIA interpretations by those authors were based on sedimentological or terrestrial analysis that included results from dating techniques. Our interpretations are based only on geomorphology and therefore chronology assessments are necessary to support this argument. Another possibility is that some of these features are younger than LIA. Cook et al. (2014) mapped the glacier front of several bays in the AP and some of the glacier front lines coincide with the location of transverse landforms (Fig. 12c, g, h) in small bays. To our knowledge, no sediment samples have been collected from any of these proximal locations and thus no chronometric data have been completed to verify the ages of these transverse features.

6 Summary and Conclusions

We present multibeam swath bathymetry from bays in the South Shetland Islands and the western Antarctic Peninsula. The subglacial landforms were classified into three categories based on their depositional environment and sedimentary processes forming them: subglacial, ice-marginal, and recent sediment reworking. We propose a schematic model showing geomorphic features present in western AP bays; from glacial lineations and moraines in the inner bay, to grounding zone wedges and drumlinoid features in the middle bay, and streamlined features and meltwater channels in the outer bay areas.

We analysed the local variables of each bay including latitude, bay area, bay length, bay width, glacier catchment area, and the seafloor lithology to understand controls on ice flow behaviour. Specific results include the following: 1) bay length and width exert a control on the number of landform features found in the bays, in addition, the geometry of the bays dictates the types of features that will form. Narrower bays tend to form transverse-to-flow features because the lateral drag of the ice flow increases as the valley width narrows which may lead to ice flow stabilization; 2) small size features, e.g. moraines were only found in narrow bays with smaller drainage areas, and not in larger-sized drainages areas, suggesting that short-lived environmental fluctuations, responsible for the formation of these features, would only be recorded by the smaller glacial systems; and 3) two different types of meltwater channels were identified: straight, wide channels carved in soft sediment are a modern erosional feature, while the complex network of channels carved in bedrock are subglacial, which highlights the presence of subglacial meltwater production in the northern AP region, possibly through several glacial cycles.

- **Deleted:**
- **Deleted:** and
- **Deleted:** , evidently,
- **Deleted:** four
- **Deleted:** glacial retreat and minor re-advance events,
- **Deleted:** flutings
- **Deleted:** s
- **Deleted:** ¶
- **Deleted:** B
- **Deleted:** .
- **Deleted:** ¶ 2) The shallowest bays analysed show signs of rapid glacial decoupling from the seafloor and subsequent retreat, which emphasizes the role of water depth as a control on ice flow.¶ 3
- **Deleted:** S
- **Deleted:** ex.
- **Deleted:** and crevasse squeeze ridges
- **Deleted:** .
- **Deleted:** ¶ 4
- **Deleted:** T
- **Deleted:** linear

Finally, based on analogous assemblages of landforms reported in other locations, we propose the geomorphic features found in the seafloor of some of the proximal bay areas were formed during the Little Ice Age glacial advance. If this is the case, then glacier systems in the AP have a greater sensitivity to minor atmospheric and oceanic fluctuations than previously suggested. Future research should include additional multibeam coverage as well as sedimentological analysis and chronometric constraints in order to confirm LIA in these bays and in other areas of the Antarctic Peninsula.

Deleted: Recently, Cook et al. (2016) concluded that glaciers in contact with warmer ocean water have retreated significantly in the AP region. The presence of deep channels in the outer bay areas may act as conduits to facilitate intrusion of deep, warm water into the inner bays causing basal melting of the tidewater glaciers.

Deleted: features

Deleted: inner

Deleted: more

Acknowledgments

This research was funded by the National Science Foundation, Office of Polar Programs grant no. OPP0739596. YPM was supported by a National Science Foundation Graduate Research Fellowship. We thank the crew and science parties of the RV/IB *Nathaniel B. Palmer* and *Araon* cruises to the Antarctic Peninsula. Data included in this study was collected during cruises NBP0201, NBP0502, NBP0602A, NBP0703, NBP1001, NBP1203, and ARA1304. NBP1001 and NBP1203 as part of the LARISSA program. We specially thank Dr. Kyu-Cheul Yoo for data from ARA1304. We would also like to thank A.G.C. Graham and S.J. Livingstone for their insightful reviews and comments which greatly improved our manuscript.

References

Alley, R.B., Anandakrishnan, S., Dupont, T.K., Parizek, B.R., and Pollard, D.: Effect of sedimentation on ice-sheet grounding-line stability, Science, 315, 1838-1841, doi:10.1126/science.1138396, 2007.

Deleted: Adie R.J: Geologic map of Antarctica, northern Antarctic Peninsula. Sheet 1, plate 1, folio 12. Geology. Antarctic Map Folio Series, American Geographical Society, New York, 1969.¶

Alley, R.B., Blankenship, D.D., Rooney, S.T., and Bentley, C.R.: Sedimentation beneath ice shelves- The view from ice stream B, Marine Geology, 85, 101-120, 1989.

Anderson, J.B.: Antarctic Marine Geology, Cambridge University Press, New York, 1999.

Anderson, J.B. and Fretwell, L.O.: Geomorphology of the onset area of a paleo-ice stream, Marguerite Bay, Antarctic Peninsula, Earth Surface Processes and Landforms, 33, 503-512, 2008.

Anderson, J.B., Wellner, J.S., Lowe, A.L., Mosola, A.B., and Shipp, S.S.: Footprint of the expanded West Antarctic Ice Sheet: ice stream history and behavior, Geol. Soc. Am. Today 11, 4–9, 2001.

Arndt, J. E., Schenke, H.W., Jakobsson, M., Nitsche, F.O., Buys, G., Goleby, B., Rebesco, M., Bohoyo, F., Hong, J., Black, J., Greku, R., Udintsev, G., Barrios, F., Reynoso-Peralta, W., Taisei, M., and Wigley, R.: The International Bathymetric Chart of the Southern Ocean (IBCSO) Version 1.0 - A new bathymetric compilation covering circumAntarctic waters, Geophysical Research Letters, 40, 3111-3117, 2013.

Deleted: Antarctic Treaty Consultative Meeting, Final Report of the Thirty-eighth Antarctic Treaty Consultative Meeting, Sofia, Bulgaria, Volume II, 121-135, 2015. ¶

Ashley, G.M. and Smith, N.D.: Marine sedimentation at a calving glacier margin, Geol. Soc. Am. Bull., 112, 657-667, 2000.

Batchelor, C.L. and Dowdeswell, J.A.: Ice-sheet grounding zone wedges (GZWs) on high-latitude continental margins, Mar. Geol., 363, 65-92, doi:10.1016/j.margeo.2015.02.001, 2015.

Bennett, M. and Glasser, N.: Glacial Geology: ice sheets and landforms, Wiley-Blackwell, UK, 2009.

Boldt, K.V., Nittrouer, C.A., Hallet, B., Koppes, M.N., Forrest, B.K., Wellner, J.S., and Anderson, J.B.: Modern rates of glacial sediment accumulation along a 15° S–N transect in fjords from the Antarctic Peninsula to southern Chile, J. Geophysical Research—Earth Surface, 118, 2072–2088, 2013.

Bradwell, T., Stoker, M., and Krabbendam, M.: Megagrooves and streamlined bedrock in NW Scotland: the role of ice streams in landscape evolution, Geomorphology, 97, 135-156, 2008.

Campo, J.M., Wellner, J.S., Domack, E., Lavoie, C., and Yoo, K.C.: Glacial geomorphology of the northwestern Weddell Sea, eastern Antarctic Peninsula continental shelf: Shifting ice flow patterns during deglaciation, Geomorphology, 280, 89-107, 2017.

Canals, M., Urgeles, R., and Calafat, A.M.: Deep sea-floor evidence of past ice streams off the Antarctic Peninsula, Geology, 28, 31-34, 2000.

Canals, M., Casamor, J.L., Urgeles, R., Calafat, A.M., Domack, E.W., Baraza, J., FArran, M., and DeBatist, M.: Seafloor evidence of a subglacial sedimentary system off the northern Antarctic Peninsula, Geology, 30, 603-604, 2002.

Christ, A.J., Talaia-Murray, M., Elking, N., Domack, E.W., Leventer, A., Lavoie, C., Brachfeld, S., Yoo, K., Gilbert, R., Jeong, S., Petrushak, S., Wellner, J., and the LARISSA group: Late Holocene glacial advance and ice shelf growth in Barilari Bay, Graham Land, west Antarctic Peninsula, Geol. Soc. Am. Bull., 127.1-2, 297-315, doi: 10.1130/B31035.1, 2014.

Cook, A.J. and Vaughan, D.G.: Overview of areal changes of the ice shelves on the Antarctic Peninsula over the past 50 - years, The Cryosphere, 4, 77-98, 2010.

Cook, A.J., Vaughan, D.G., Luckman, A.J., and Murray, T.: A new Antarctic Peninsula glacier basin inventory and observed area changes since the 1940s, Antarctic Science, 26, 614-624, 2014.

Deleted: Cook, A.J., Holland, P.R., Meredith, M.P., Murray, T., Luckman, A., and Vaughan, D.G.: Ocean forcing of glacier retreat in the western Antarctic Peninsula, Science, 353, 283-286, 2016. ¶

Domack, E.W.: Laminated terrigenous sediments from the Antarctic Peninsula: the role of subglacial and marine processes, In Dowdeswell, J.A. and Scourse, J.D. (eds.) Glaciomarine environments: processes and sediments, Geological Society Special Publication, 53, 91-103, 1990.

Domack, E.W. and Ishman, S.: Oceanographic and physiographic controls on modern sedimentation within Antarctic fjords, Geol. Soc. Am. Bull., 105, 1175-1189, 1993.

Domack, E.W., Foss, D.J.P., Syvitski, J.P.M., and McClennen, C.E.: Transport of suspended particulate matter in an Antarctic fjord, Marine Geology, 121, 161-170, 1994.

Domack, E.W., Ishman, S.E., Stein, A.B., McClennen, C.E., and Jull, A.J.T.: Late Holocene advance of the Muller Ice Shelf, Antarctic Peninsula: sedimentological, geochemical, and palaeontological evidence, Antarctic Science, 7, 159-170, 1995.

Domack, E.W., Leventer, A., Dunbar, R., Taylor, F., Brachfeld, S., Sjuunneskog, C., and ODP Leg 178 Scientific Party: Chronology of the Palmer Deep site, Antarctic Peninsula: a Holocene palaeoenvironmental reference for the circum-Antarctic, The Holocene, 11, 1-9, 2001.

Domack, E.W., Leventer, A., Root, S., Ring, J., Williams, E., Carlson, D., Hirshorn, E., Wright, W., Gilbert, R., and Burr, G.: Marine sedimentary record of natural environmental variability and recent warming in the Antarctic Peninsula, in: Antarctic Peninsula Climate Variability, Antarctic Research Series, edited by: Domack, E., 79, 205-224, doi:10.1029/079ARS17, 2003.

Domack, E., Amblas, D., Gilbert, R., Brachfeld, S., Camerlenghi, A., Rebesco, M., Canals, M., and Urgeles, R.: Subglacial morphology and glacial evolution of the Palmer deep outlet system, Antarctic Peninsula, Geomorphology, 75, 125-142, 2006.

Dowdeswell, J.A. and Vasquez, M.: Submarine landforms in the fjords of southern Chile: implications for glacimarine processes and sedimentation in a mild glacier-influenced environment, Quaternary Science Reviews, 64, 1-19, http://dx.doi.org/10.1016/j.quascirev.2012.12.003, 2013.

Dowdeswell, J.A., ÓCofaigh, C., and Pudsey, C.J.: Continental slope morphology and sedimentary processes at the mouth of an Antarctic palaeo-ice stream, Marine Geology, 204, 203-214, 2004.

Dowdeswell, J.A., Ottesen, D., Evans, J., OCofaigh, C., and Anderson, J.B.: Submarine glacial landforms and rates of ice-stream collapse, Geology, 36, 819-822, doi: 10.1130/G24808A, 2008.

Dowdeswell, J.A., Hogan, K.A., Evans, J., Noormets, R., ÓCofaigh, C., Ottesen, D.: Past-ice sheet flow east of Svalbard inferred from streamlined subglacial landforms, Geology, 38, 163-166, doi: 10.1130/G30621.1, 2010.

Dowdeswell, J. A., Hogan, K.A., and ÓCofaigh, C.: Submarine glacial-landform distribution across the West Greenland margin: a fjord-shelf-slope transect through the Uummannaq system (70° to 71° N), in: Atlas of Submarine Glacial Landforms: Modern, Quaternary and Ancient, edited by Dowdeswell J.A., Canals, M., Jakobsson, M, Todd, B.J., Dowdeswell, E.K., and Hogan, K.A., Geol. Soc. Lond. Memoirs, 46, 1-4, doi: 10.1144/M46.168, 2016.

Evans, J., Dowdeswell, J.A., ÓCofaigh, C.: Late Quaternary submarine bedforms and ice-sheet flow in Gerlache Strait and on the adjacent continental shelf, Antarctic Peninsula, J. Quaternary Science, 19, 397-407, doi:10.1002/jqs.831, 2004.

Fernandez, R.A., Anderson, J.B., Wellner, J.S., Minzoni, R.L., Halet, B., and Smith, R.T.: Latitudinal variation in glacial erosion rates from Patagonia and the Antarctic Peninsula (46°S-65°S), Geol. Soc. Am. Bull., 128, 1000-1023, doi: 10.1130/B31321.1, 2016.

Fox, A.J. and Cooper A.P.R.: Climate-change indicators from archival aerial photography of the Antarctic Peninsula, Annals of Glaciology, 27, 636-642, 1998.

Fretwell, P., Pritchard, H.D., Vaughan, D.G., Bamber, J.L., Barrand, N.E., Bell, R., Bianchi, C., Bingham, R.G., Blankenship, D.D., Casassa, G., Catania, G., Callens, D., Conway, H., Cook, A.J., Corr, H.F.J., Damaske, D., Damm, V., Ferraccioli, F., Forsberg, R., Fujita, S., Gim, Y., Gogineni, P., Griggs, J.A., Hindmarsh, R.C.A., Holmlund, P., Holt, J.W., Jacobel, R.W., Jenkins, A., Jokat, W., Jordan, T., King, E.C., Kohler, J., Krabill, W., Riger-Kusk, M., Langley, K.A., Leitchenkov, G., Leuschen, C., Luyendyk, B.P., Matsuoka, K., Mouginot, J., Nitsche, F.O., Nogi, Y., Nost, O.A., Popov, S.V., Rignot, E., Rippin, D.M., Rivera, A., Roberts, J., Ross, N., Siegert, M.J., Smith, A.M., Steinhage, D., Studinger, M., Sun, B., Tinto, B.K., Welch, B.C., Wilson, D., Young. D.A., Xiangbin, C., and Zirizzotti, A.: Bedmap2: improved ice bed, surface and thickness datasets for Antarctica, The Cryosphere 7, 375-393, 2013.

Gales, J.A., Larter, R.D., Mitchell, N.C., and Dowdeswell, J.A.: Geomorphic signature of Antarctic submarine gullies: implications for continental slope processes, Marine Geology, doi: 10.1016/j.margeo.2013.02.003, 2013.

Garcia, M., Dowdeswell, J.A., Noormets, R., Hogan, K.A., Evans, J., ÓCofaigh, C., and Larter, R.D.: Geomorphology and shallow-acoustic investigation of an Antarctic Peninsula fjord system using high resolution ROV and shipboard geophysical observations: ice dynamics and behaviour since the Last Glacial Maximum, Quaternary Science Reviews, 153, 122-138, http://dx.doi.org/10.1016/j.quascirev.2016.10.014, 2016.

Graham, A.G.C., Kuhn, G., Meisel, O., Hillenbrand, C.D., Hodgson, D. A., Ehrmann, W., Wacker, P., Wintersteller, P., Ferreira, C.D.S., Romer, M., White, D., and Bohrmann, G.: Major advance of South Georgia glaciers during the Antarctic Cold Reversal following extensive sub-Antarctic glaciation, Nature Communications, 8:14798, doi:10.1038/ncomms14798, 2017.

Graham, A.G.C., Larter, R.D., Gohl, K., Hillenbrand, C.D., Smith, J.A., and Kuhn, G.: Bedform signature of a West Antarctic palaeo-ice stream revels a multi-temporal record of flow and substrate control, Quaternary Science Reviews, 28, 2774-2793, 2009.

Graham, A.G.C. and Smith, J.A.: Palaeoglaciology of the Alexander Island ice cap, western Antarctic Peninsula, reconstructed from marine geophysical and core data, Quaternary Science Reviews, 35, 63-81, 2012.

Griffith, T.W. and Anderson, J.B.: Climatic control of sedimentation in bays and fjords of the northern Antarctic Peninsula. Marine Geology, 181-204, 1989.

Halberstadt, A.R., Simkins, L.M., Greenwood, S.L., and Anderson, J.B.: Past ice-sheet behaviour: retreat scenarios and changing controls on the Ross Sea, Antarctica, The Cryosphere, 10, 1003-1020, 2016.

Hall, B.L.: Late-Holocene advance of the Collins Ice Cap, King George Island, South Shetland Islands, The Holocene, 17, 1253-1258, 2007.

Hass, H.C., Kuhn, G., Monien, P., Brumsack, H.J., and Forwick, M.: Climate fluctuations during the past two millennia as recorded in sediments from Maxwell Bay, South Shetland Islands, West Antarctica, in: Fjord systems and archives, edited by: Howe, J.A., Austin, W.E.N., Forwick, M., and Paetsel, M, Geological Society of London, 344, 243-260, doi:10.1144/SP344.17, 2010.

Heroy, D.C. and Anderson, J.B.: Ice-sheet extent of the Antarctic Peninsula region during the Last Glacial Maximum (LGM) – Insights from glacial geomorphology. Geol. Soc. Am Bull., 117, 1497-1512, 2005.

Hodgson, D. A., Graham, A.G.C., Griffiths, H.J., Roberts, S.J., Ó Cofaigh, C., Bentley, M.J., and Evans, D.J.A.: Glacial history of sub-Antarctic South Georgia based on the submarine geomorphology of its fjords, Quaternary Science Reviews, 89, 129-147, 2014.

Howat, I.M., and Domack, E.W.: Reconstructions of western Ross Sea palaeo-ice-stream grounding zones from high-resolution acoustic stratigraphy, Boreas, 32, 56-75, 2003.

Jamieson, S.S.R., Vieli, A., Livingstone, S.J., Ó Cofaigh, C., Stokes, C., Hillenbrand, C.D., and Dowdeswell, J.A.: Ice-stream stability on a reverse bed slope, Nature Geoscience, 5, 799-802, doi:10.1038/NGEO1600, 2012.

Joughin, I., Howat, I.M., Fahnestock, M., Smith, B., Krabill, W., Alley, R.B., Stern, H., and Truffer, M.: Continued evolution of Jakobshavn Isbrae following its rapid speedup, J. Geophysical Research, 113, F04006, doi:10.1029/2008JF001023, 2008.

King J.C., Turner, J., Marshall G.T., Connelley, W.M. & Lachlan-Cope, T.A.: Antarctic Peninsula climate variability and its causes as revealed by analysis of instrumental records. In Antarctic Peninsula climate variability, Domack, E, American Geophysical Union, Washington, DC, 2003.

Klages, J.P., Kuhn, G., Hillenbrand, C.D., Graham, A.G.C., Smith, J.A., Larter, R.D., and Gohl, K.: First geomorphological record and glacial history of an inter-ice stream ridge on the West Antarctic continental shelf, Quaternary Science Reviews, 61, 47-61, http://dx.doi.org/10.1016/j.quascirev.2012.11.007, 2013.

KOPRI: Annual report of environmental monitoring on human impacts around the King Sejong Station, Antarctica. Korea Polar Research Institute Report, No. BSE 413040-1-11, 2014.

Kuhn, G., Hillenbrand, C.D., Kasten, S. Smith, J.A., Nitsche, F.O., Frederichs, T., Wiers, S., Ehrmann, W., Klages, J.P., and Mogollon, J.M: Evidence for a palaeo-subglacial lake on the Antarctic continental shelf, Nature Communications, 8:15591, doi:10.1038/ncomms15591, 2017.

Lavoie, C., Domack, E.W., Pettit, E.C., Scambos, T.A., Larter, R.D., Schenke, H.W., Yoo, K.C., Gutt, J., Wellner, J., Canals, M., Anderson, J.B., and Amblas, D.: Configuration of the Northern Antarctic Peninsula Ice Sheet at LGM based on a new synthesis of seabed imagery, The Cryosphere, 9, 613-629, doi:10.5194/tc-9-613-2015, 2015.

Larter, R.D., Graham, A.G.C., Gohl, K., Kuhn, G., Hillenbrand, C.D., Smith, J.A., Deen, T.J., Livermore, R.A., Schenke, H.W.: Subglacial bedforms reveal complex basal regime in a zone of paleo-ice stream convergence, Amundsen Sea Embayment, West Antarctica, Geology, 37, 411-414, 2009.

Lee, J., Jin, Y.K., Hong, J.K., Yoo, H.J., and Shon, H.: Simulation of a tidewater glacier evolution in Marian Cove, King George Island, Antarctica, Geosciences Journal, 12, 33-39, doi:10.1007/s12303-008-0005-x, 2008.

Livingstone, S.J., Ó Cofaigh, C., Stokes, C.R., Hillenbrand, C.D., Vieli, A., and Jamieson, S.S.R.: Glacial geomorphology of Marguerite Bay palaeo-ice stream, western Antarctic Peninsula, J. Maps, 9, 558-572, http://dx.doi.org/10.1080/17445647.2013.829411, 2013.

Lowe, A.L. and Anderson, J.B.: Reconstruction of the West Antarctic ice sheet in Pine Island Bay during the Last Glacial Maximum and its subsequent retreat history, Quaternary Science Reviews, 21, 1879-1897, 2002.

Milliken, K.T., Anderson, J.B, Wellner, J.S., Bohaty, S.M., and Manley, P.L.: High resolution Holocene climate record from Maxwell Bay, South Shetland Islands, Antarctica. Geol. Soc. Am Bull., 121, 1711-1725, 2009.

Monien, P., Schnetger, B., Brumsack, H.J., Hass, H.C., and Kuhn, G.: A geochemical record of late Holocene palaeoenvironmental changes at King George Island (maritime Antarctica), Antarctic Science, 23, 255-267, doi:10.1017/S095410201100006X, 2011.

Moon, H.W., Wan Hussin, W. M. R., Kim, H.C., and Ahn, I.Y.: The impacts of climate change on Antarctic nearshore ega-epifaunal benthic assemblages in a glacial fjord on King George Island: Responses and implications, Ecological Indicators, 57, 280-292, 2015.

Morris, E.M. and Vaughan, D.G.: Spatial and temporal variation of surface temperature on the Antarctic Peninsula and the limit of variability of ice shelves, Antarctic Research Series, 79, 61-68, 2003.

Munoz, Y.P. and Wellner, J.S.: Local controls on sediment accumulation and distribution in a fjord in the West Antarctic Peninsula: implications for palaeoenvironmental interpretations, Polar Research, 35, 25284, http://dx.doi.org/10.3402/polar.v35.25284, 2016.

Nitsche, F. O., Gohl, K., Larter, R.D., Hillenbrand, C.D., Kuhn, G., Smith, J.A., Jacobs, S., Anderson, J.B., and Jakobsson, M.: Paleo ice flow and subglacial meltwater dynamics in Pine Island Bay, West Antarctica, The Cryosphere, 7, 249-262, 2013

Ó Cofaigh, C. and Dowdeswell, J.A.: Laminated sediments in glacimarine environment: diagnostic criteria for their interpretations, Quaternary Science Reviews, 20, 1411-1436, 2001.

Ó Cofaigh, C., Pudsey, C.J., Dowdeswell, J.A., and Morris, P.: Evolution of subglacial bedforms along a paleo-ice stream, Antarctic Peninsula continental shelf, Geophysical Research Letters, 29, 1199, doi:10.1029/2001GL014488, 2002.

Ó Cofaigh, C., Larter, R.D., Dowdeswell, J.D., Hillenbrand, C.D., Pudsey, C.J., Evans, J., and Morris, P.: Flow of the West Antarctic Ice Sheet on the continental margin of the Bellingshausen Sea at the Last Glacial Maximum, J. Geophysical Research, 110, B11103, doi:10.1029/2005JB003619, 2005.

Ó Cofaigh, C., Davies, B.J., Livingstone, S.T., Smith, J.A., Johnson, J.S., Hocking, E.P., Hodgson, D.A., Anderson, J.B., Bentley, M. J., Canals, M., Domack, E., Dowdeswell, J.D., Evans, J., Glasser, N.F., Hillenbrand, C.D., Larter, R.D., Roberts, S.J., and Simms, A.: Reconstruction of ice-sheet changes in the Antarctic Peninsula since the Last Glacial Maximum, Quaternary Science Reviews, 100, 87-110, 2014.

O'Neel, S., Pfeffer, W.T., Krimmel, R., and Meier, M.: Evolving force balance a Columbia Glacier, Alaska, during its rapid retreat, J. Geophysical Research, 110, F03012, doi:10.1029/2005JF000292, 2005.

Ottesen, D. and Dowdeswell, J.A.: Assemblages of submarine landforms produced by tidewater glaciers in Svalbard, J. Geophysical Research, 111, F01016, doi:10.1029/2005JF000330, 2006.

Ottesen, D. and Dowdeswell, J.A.: An inter-ice-stream glaciated margin: Submarine landforms and a geomorphic model based on marine geophysical data from Svalbard, Geol. Soc. Am. Bull., 121, 1647-1665, doi:10.1130/B26467.1, 2009.

Ottesen, D., Dowdeswell, J.A., and Rise, L.: Submarine landforms and the reconstruction of fast-flowing ice streams within a large Quaternary ice sheet: The 2500-km-long Norwegian-Svalbard margin (57°-80°N), Geol. Soc. Am. Bull. 117, 1033-1050, doi: 10.1130/B25577.1, 2005.

Pereira, T.T.C., Schaefer, C.E.G.R., Ker, J.C., Almeida, C.C., Almeida, I.C.C., and Pereira, A.B.: Genesis, mineralogy and ecological significance of ornithogenic soils from a semi-desert polar landscape at Hope Bay, Antarctic Peninsula, Geoderma, 209-210, 98-109, http://dx.doi.org/10.1016/j.geoderma.2013.06.012, 2013.

Powell, R.D.: A model for sedimentation by tidewater glaciers, Annals of Glaciology 2, 129-134, 1981.

Powell, R.D., and Domack, E.W.: Modern glaciomarine environments, In J. Menzies (ed.) Modern glacial environments: processes, dynamics, and sediments, Boston, Butterworth-Heinmann, 445-486, 1995.

Robel, A.A.: Thinning sea ice weakens buttressing force of iceberg melange and promotes calving, Nature Communications, 8, 14596, doi:10.1038/ncomms14596, 2017.

Ruckamp, M., Braun, M., Suckro, S. and Blindow, N.: Observed glacial changes on the King George Island ice cap, Antarctica, in the last decade, Global and Planetary Change, 79, 99-109, doi:10.1016/j.gloplacha.2011.06.009, 2011.

Schaefer, C.E.G.R., Pereira, T.T.C., Almeida, I.C.C., Michel, R.F.M., Correa, G.R., Figueiredo, L.P.S., and Ker, J.C.: Penguin activity modify the thermal regime of active layer in Antarctica: A case study from Hope Bay, Catena, http://dx.doi.org/10.1016/j.catena.2016.07.021, 2016.

Shevenell, A.E., Domack, E.W., and Kernan, M.: Record of Holocene palaeoclimate change along the Antarctic Peninsula: evidence from glacial marine sediments, Lallemand Fjord, in: Climatic succession and glacial history of the southern hemisphere over the last five million years, edited by: Banks, M.R., and Brown, M.J., Papers and Proceedings of the Royal Society of Tasmania, 130, 55-64, 1996.

Simms, A.R., Milliken, K.T., Anderson, J.B., and Wellner, J.S.: The marine record of deglaciation of the South Shetland Islands, Antarctica since the Last Glacial Maximum, Quaternary Science Reviews, 30, 1583-1601, doi:10.1016/j.quascirev.2011.03.018, 2011.

Simms, A.R., Ivins, E.R., DeWitt, R., Kouremenos, P., and Simkins, L.M.: Timing of the most recent Neoglacial advance and retreat in the South Shetland Islands, Antarctic Peninsula, insights from raised beaches and Holocene uplift rates, Quaternary Science Reviews, 47, 41-55, doi:10.1016/j.quascirev.2012.05.013, 2012.

Syvitski, J.P.M., Burrell, D.C., and Skei, J.M.: Fjords: processes and products, Springer, Berlin, 1987.

Turner, J., Lu, H., White, I., King, J.C., Phillips, T., Hosking, J.S., Bracegirdle, T.J., Marshall, G.J., Mulvaney, R., and Deb, P.: Absence of 21st century warming on Antarctic Peninsula consistent with natural variability, Nature Letter, 535, 411-415, 2016.

Thomas, E.R., Marshall, G.J., and McConnell, J.R.: A doubling in snow accumulation in the western Antarctic Peninsula since 1850, Geophysical Research Letters, 35, L01706, doi:10.1029/2007GL032529, 2008

Wellner, J.S., Lowe, A.L., Shipp, S.S., and Anderson, J.B.: Distribution of glacial geomorphic features on the Antarctic continental shelf and correlation with substrate: implications for ice behavior, J. Glaciol., 47, 397-411, doi:10.3189/172756501781832043, 2001.

Wellner, J.S., Heroy, B.C., and Anderson, J.B.: The death mask of the Antarctic ice sheet: comparison of glacial geomorphic features across the continental shelf, Geomorphology, 75, 157–171, doi:10.1016/j.geomorph.2005.05.015, 2006.

Whillans, I.M. and van deer Veen, C.J.: The role of lateral drag in the dynamics of Ice Stream B, Antarctica, J. Glaciology, 43, 231-237, 1997.

Wolfl, A.C., Wittenberg, N., Feldens, P., Hass, H.C., Betzler, C., and Kuhn, G.: Submarine landforms related to glacier retreat in a shallow Antarctic fjord, Antarctic Science, 1-12, doi:10.1017/S0954102016000262, 2016.

Yoon, H.I., Yoo, K.C., Park, B.K., Kim, Y., Khim, B.K., and Kang, C.Y.: The origin of massive diamicton in Marian and Potter coves, King George Island, West Antarctica, Geosciences Journal, 8, 1-10, 2004.

Deleted: ¶

Formatted: Font: English (United States)

Figures

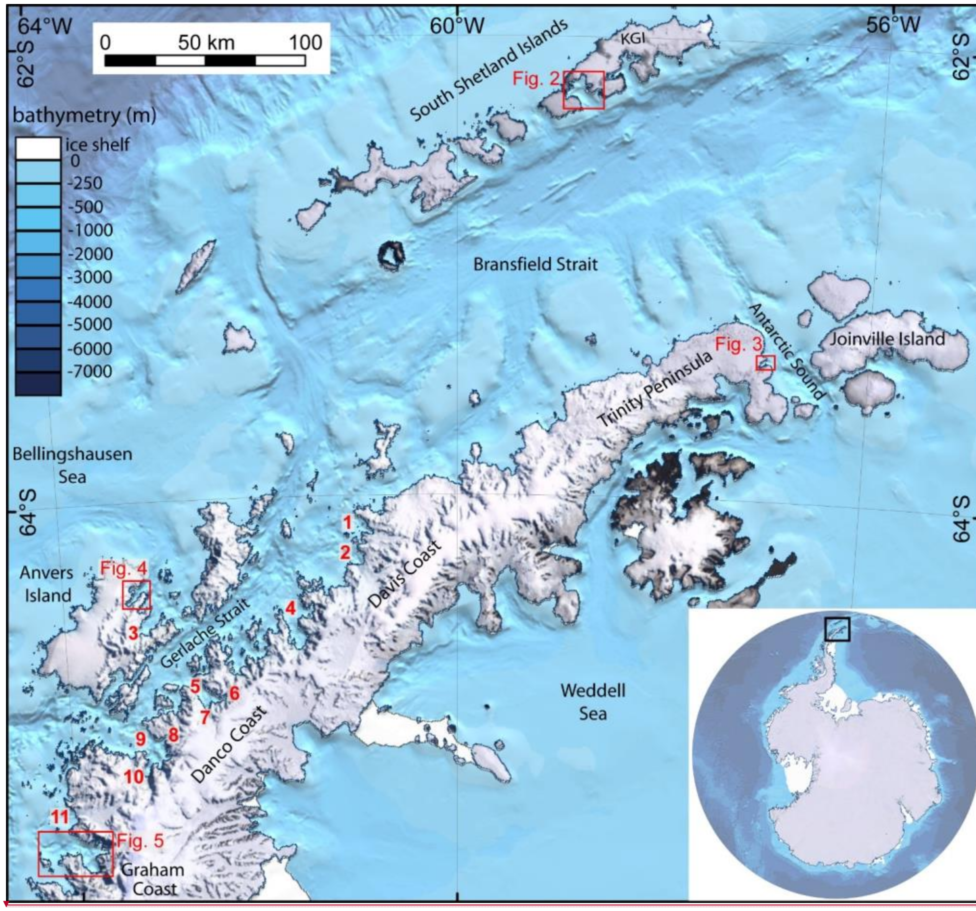

Figure 1. Map of the northern Antarctic Peninsula (AP) and South Shetland Islands, red boxes indicate Figures 2-5. Inset shows the location of the AP in Antarctica. KGI: King George Island, 1 Cierva Cove, 2 Brialmont Cove, 3 Fournier Bay, 4 Charlotte Bay, 5 Andvord Bay, 6 Moser Glacier 7 Lester Cove, 8 Briand Fjord, 9 Flandres Bay, 10 Etienne Fjord, 11 Collins Bay. Individual maps of bays 1-11 found in the supplementary material. AP map from Polar Geospatial Center, bathymetry and inset from IBCSO (Arndt et al., 2013).

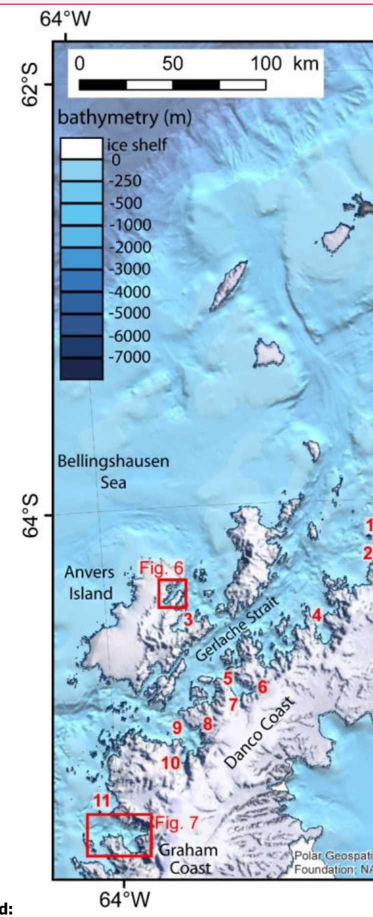

Deleted:

Formatted: Keep with next

Formatted: English (United States)

Formatted: Font: 10 pt

Formatted: Caption, Left

Formatted ...

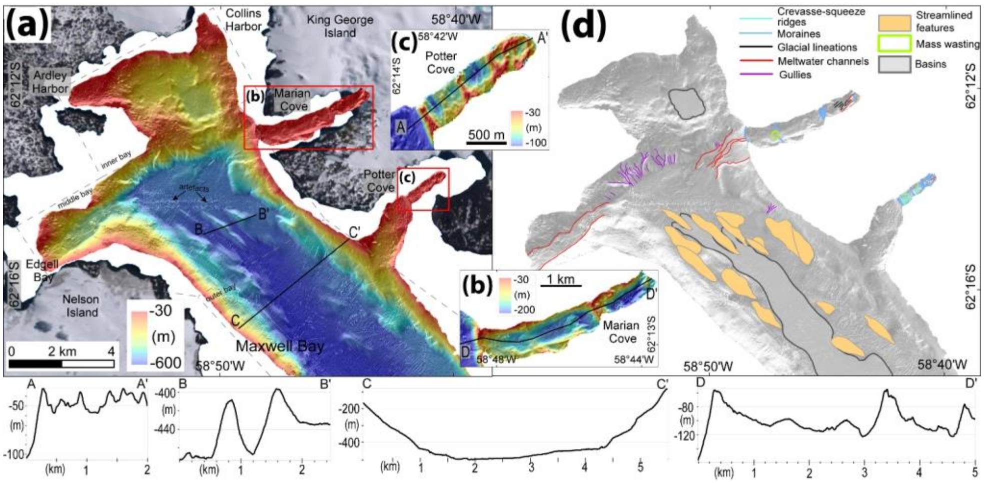

Figure 2. Multibeam swath bathymetry of Maxwell Bay (a), Marian Cove (b), and Potter Cove (c), vertical exaggeration is 5x in all images. (d) Interpretation of geomorphic features with hillshade as background. Cross sections A-A' and D-D' show transverse ridges in Potter Cove (c) and Marian Cove (b) respectively, B-B' shows elongated ridges in the bay, C-C' shows the U-shaped fjord valley.

Formatted: Keep with next

Formatted: Left

Formatted: Font: 10 pt, Not Bold

Formatted: Normal

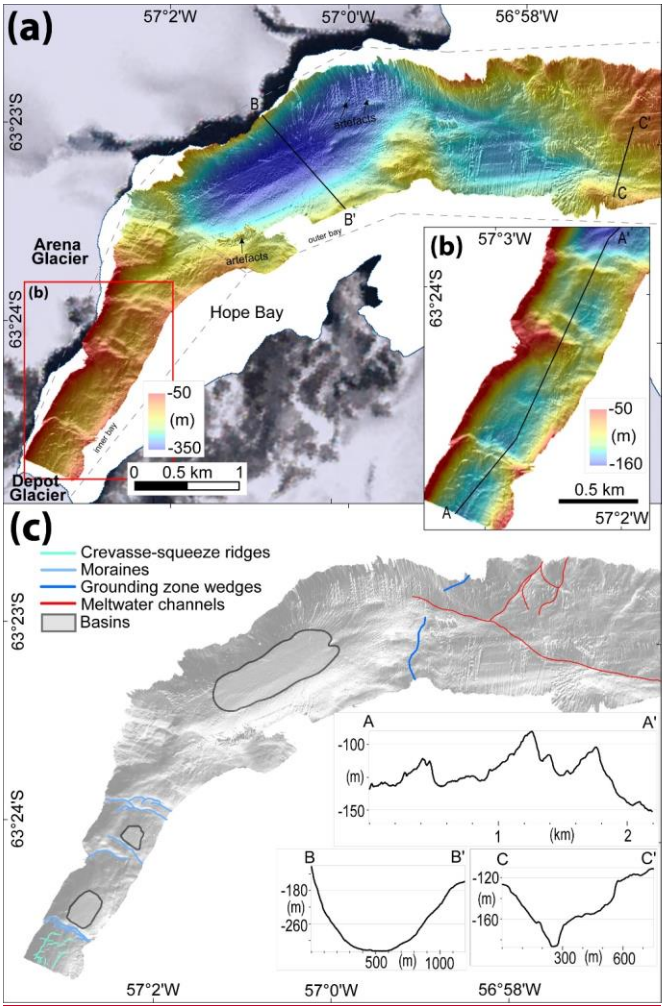

Figure 3. Multibeam swath bathymetry of Hope Bay (a), the inner bay area (b), and interpretation of geomorphic features with hillshade as background (c). Transverse ridges can be seen in A-A', the U-shaped fjord valley is seen in B-B', and a meltwater channel in the outer bay (C-C'). Vertical exaggeration is 3x in all images.

Formatted: Left

Formatted: Normal

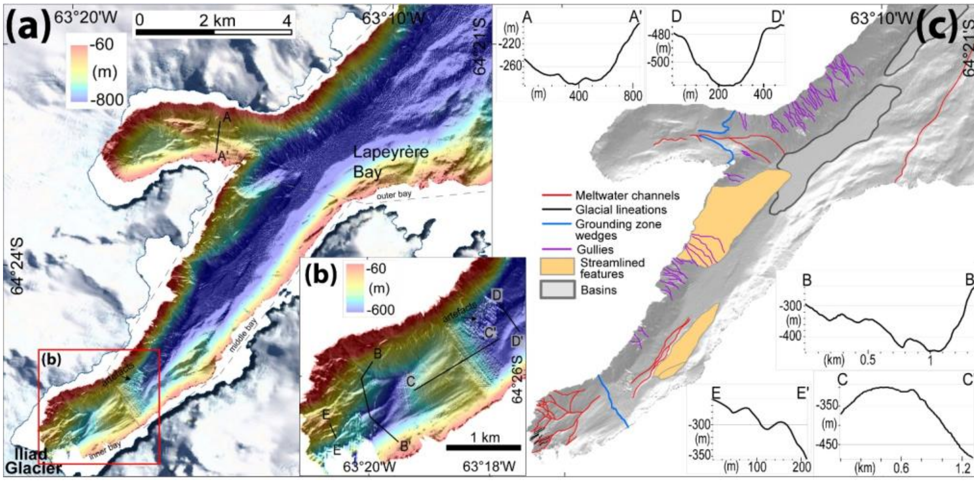

Figure 4. Multibeam swath bathymetry of Lapeyrère Bay (a), the inner bay area (b), and the interpretation of geomorphic features with hillshade as background (c). Cross section A-A', B-B', and D-D' show meltwater channels around the bay, C-C' shows the grounding zone wedge in the inner bay, and E-E' show glacial lineations in the inner bay area. Vertical exaggeration is 5x in (a) and 3x in (b).

Formatted: Keep with next

Formatted: Font: 10 pt, Not Bold

Formatted: Normal

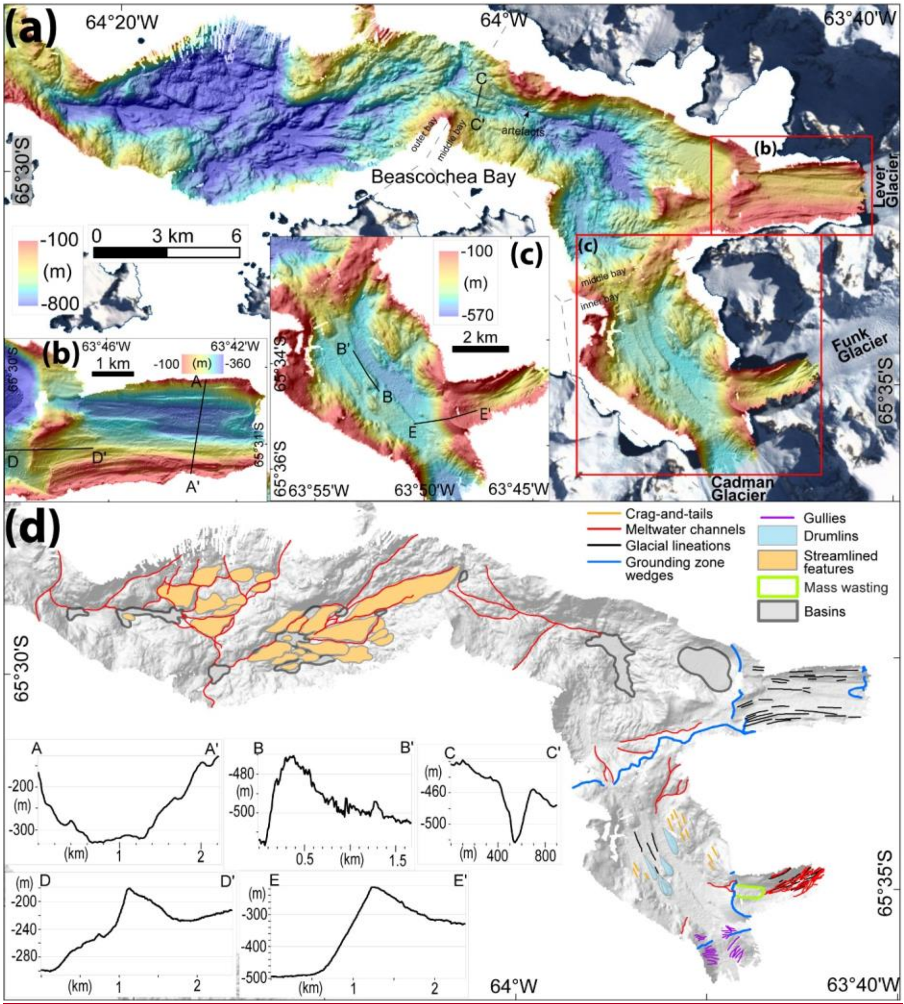

Figure 5. Multibeam swath bathymetry of Beascochea Bay (a), Lever Glacier cove (b), the inner bay area (c), and the interpretation of geomorphic features with hillshade as background (d). A-A' shows glacial lineations in Lever Glacier cove, B-B' show a drumlin in the inner bay area, C-C' show the cross-section profile of a meltwater channel, D-D' and E-E' show large transverse ridges. Vertical exaggeration is 3x in all images.

Formatted: Justified

Deleted: Figure 1: Map of the northern Antarctic Peninsula (AP) and South Shetland Islands, red boxes indicate Figures 4-7. Inset shows the location of the AP in Antarctica. 1 Cierva Cove, 2 Brialmont Cove, 3 Fournier Bay, 4 Charlotte Bay, 5 Anvord Bay, 6 Moser Glacier 7 Lester Cove, 8 Briand Fjord, 9 Flandres Bay, 10 Etienne Fjord, 11 Collins Bay. AP map from Polar Geospatial Center, bathymetry and inset from IBCSO (Arndt et al., 2013).

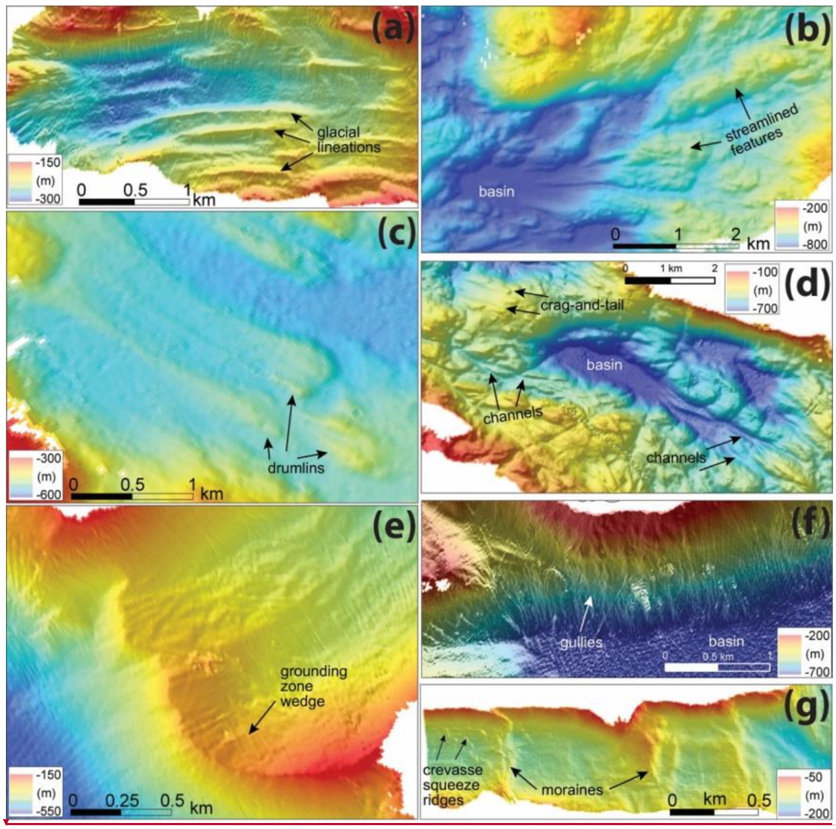

Figure 6. Seafloor landforms found in the bays of the western Antarctic Peninsula: (a) glacial lineations, (b) streamlined features and basin, (c) drumlins, (d) crag-and-tails, meltwater channels, and basin, (e) grounding zone wedge, (f) gullies and basin, (g) moraines and crevasse squeeze ridges.

Deleted:

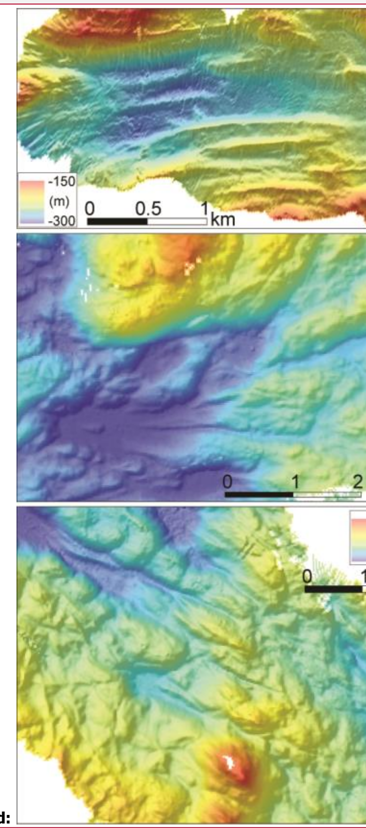

Deleted: ¶

Figure 2: Seafloor landforms found in the bays of the western Antarctic Peninsula: (a) flutings, (b) moraine and crevasse squeeze ridges, (c) streamlined features, (d) drumlins, (e) channels, (f) grounding zone wedge.¶

Facies	Description	Interpretation	CHIRP example	Multibeam example
1	acoustically layered, parallel reflectors	glaciomarine sediments infilling basins	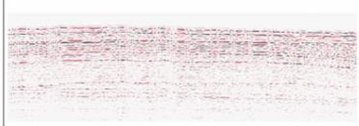	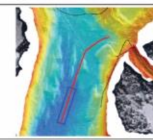
2	bowtie or hummocky, chaotic reflectors	bedrock		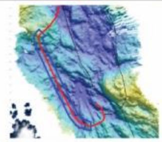
3	strong surface, little to no acoustic penetration	till and/or bedrock		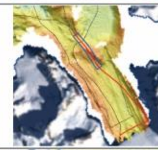
4	thin, acoustically semi-transparent drape, overlying a strong reflector	thin, fine-grained sediment cover	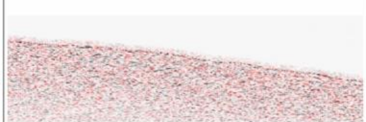	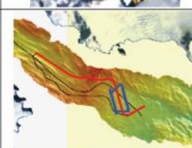
5	weak reflector, mound shape	slump, debris flow deposits		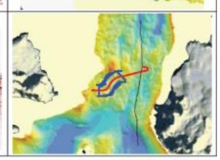

Localised examples:

(a) Asymmetric wedge with reflections: thin sediment cover, drumlin	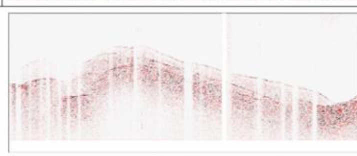	
(b) Stacked sediment packages: channel-glacial lineation pair, near ice front	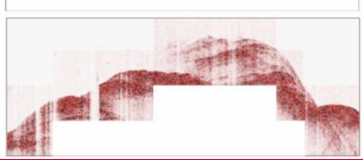	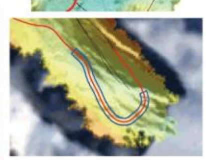

Figure 7. CHIRP facies showing seafloor lithology. Five facies were identified throughout the bay, in addition, two localized examples of features are shown: (a) drumlin and (b) glacial lineations near the modern ice front. The blue rectangle in multibeam example shows the location of the chirp example shown.

Deleted:

facies	description	interpretation
1	Thinly layered	Basin fill
2	Bowtie or hummocky reflections	Bedrock
3	Strong surface, no internal reflectors	Till
4	Thin layer covering a strong reflector	Thin, fine-grained sediment cover
5	Weak reflections, mount shape	Slump, debris flow deposits

Localized examples

(a) Asymmetric wedge with reflections: thin sediment cover, drumlin

(b) Stacked sediment packages: channel-fluting pair, near ice front

Formatted: English (United States)

Formatted: Caption, Left

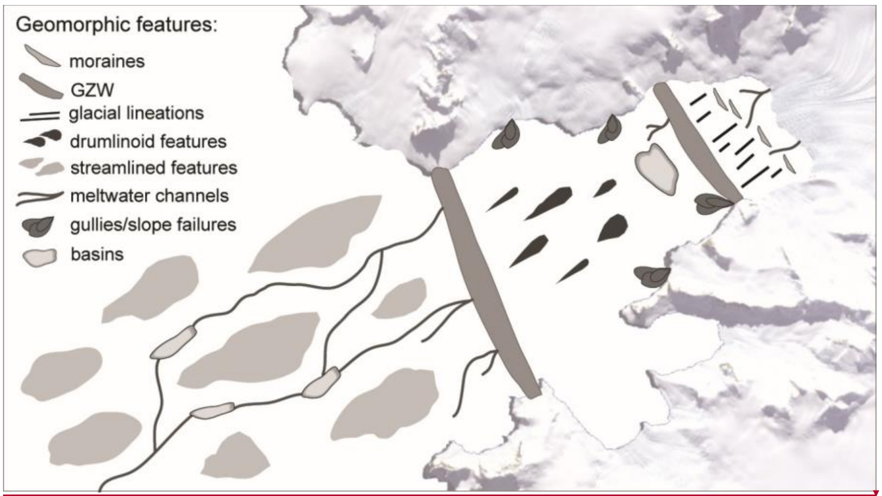

Figure 8. Schematic map view model showing the various geomorphic features found in the seafloor of glaciated bays in the western Antarctic Peninsula.

Deleted: ¶
Figure 3: Chirp facies showing seafloor lithology. Five facies were identified throughout the bay, in addition, two localized examples of features are shown: (a) drumlin and (b) flutings near the modern ice front. The blue rectangle in multibeam example shows the location of the chirp example shown. ¶
¶

Deleted: ¶

Deleted: ¶

Formatted: Normal

Deleted: Figure 5: Multibeam swath bathymetry of Hope Bay, see Fig. 1 for location. The inner bay is shown in (b), moraines can be seen in A-A', the U-shaped fjord valley is seen in B-B', and a meltwater channel in the outer bay (C-C'). Vertical exaggeration is 3x in both images.¶
¶

Deleted: ¶
Figure 8: Schematic map view model showing the various geomorphic features found in the seafloor of glaciated bays in the western Antarctic Peninsula.¶

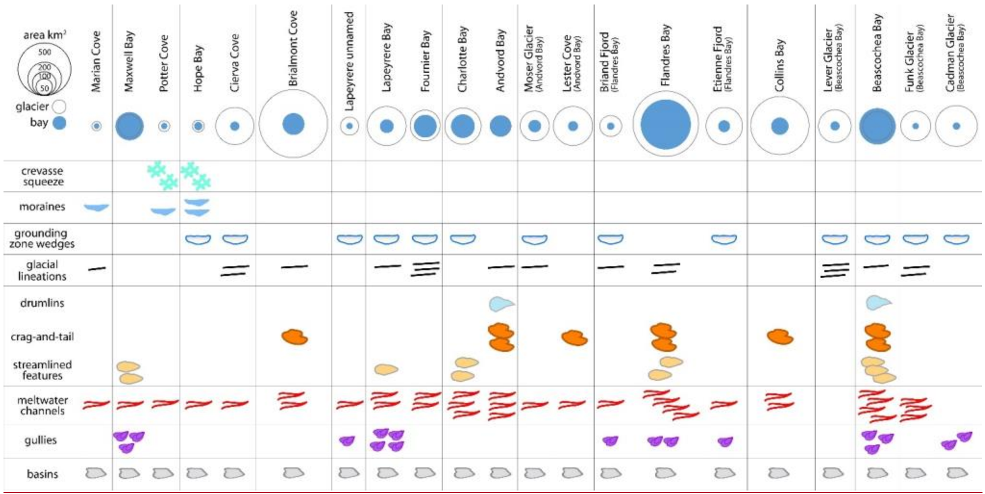

Figure 9. Comparing bay area, glacier catchment area, and submarine features found in bays. Bays are listed from northernmost (Marian Cove) to southernmost (Cadman Glacier Cove). The number of symbols in the chart is a representation of the number of geomorphic features found in each bay; one symbol: 1-10 features; two symbols: 11-20 features; three symbols: 21-30 features; and four symbols: >30 features found at that location.

Deleted: ¶

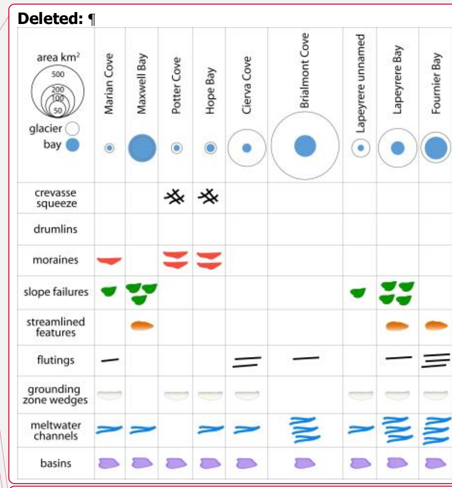

Formatted: Font: Not Bold

Deleted: ¶
Figure 9: Comparing bay area, glacier catchment area, and submarine features found in bays. Bays are listed from northernmost (Marian Cove) to southernmost (Cadman Glacier Cove). The number of symbols in the chart is a representation of the number of geomorphic features found in each bay: one symbol represents less than 10 features, two symbols represents between 10 and 20, three symbols represents between 20 and 30, and four symbols represents greater than 30 features found at that location.¶

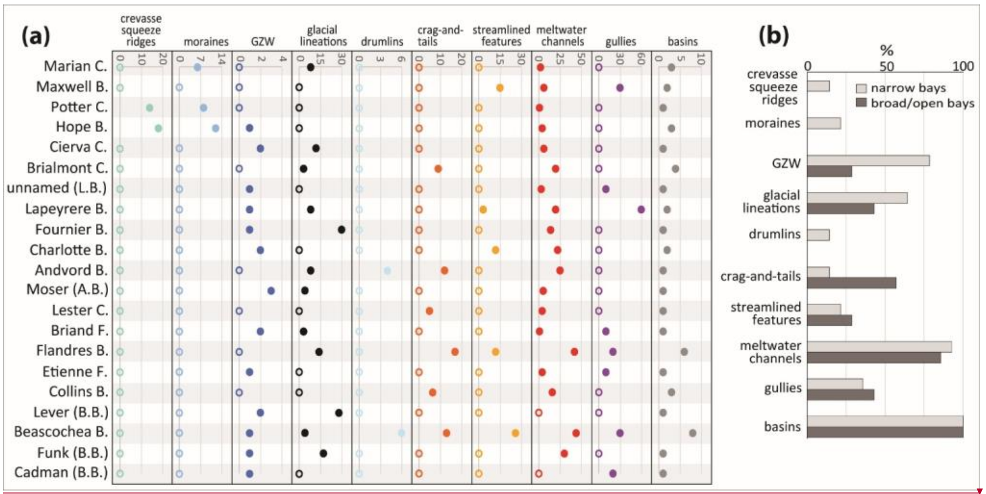

Figure 10. (a) Number of features found in the bays, open circles represent zero; the bays are listed from northernmost to southernmost latitude; C.: cove, B.: bay, F.: fjord, L.B.: Lapeyrère Bay, A.B.: Andvord Bay, B.B.: Beascochea Bay. (b) Percent of narrow (light grey) and broad/open bays (dark grey) in which the listed geomorphic features are found.

Deleted:

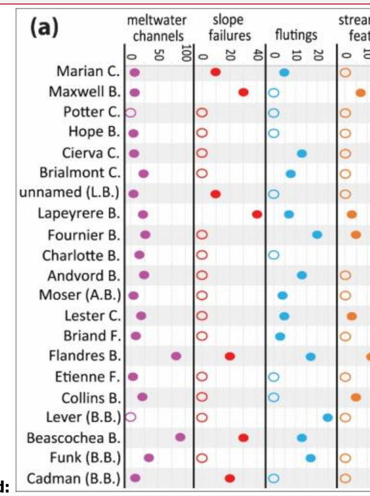

Formatted: Caption, Left

Deleted: ¶

Figure 10: (a) Number of features found in the bays, open circles represent zero; the bays are listed from northernmost to southernmost latitude; C. cove, B. bay, F. fjord, L.B. Lapeyrère Bay, A.B. Andvord Bay, B.B. Beascochea Bay. (b) Percent of narrow (light grey) and broad/open bays (dark grey) in which the listed geomorphic features are found. ¶

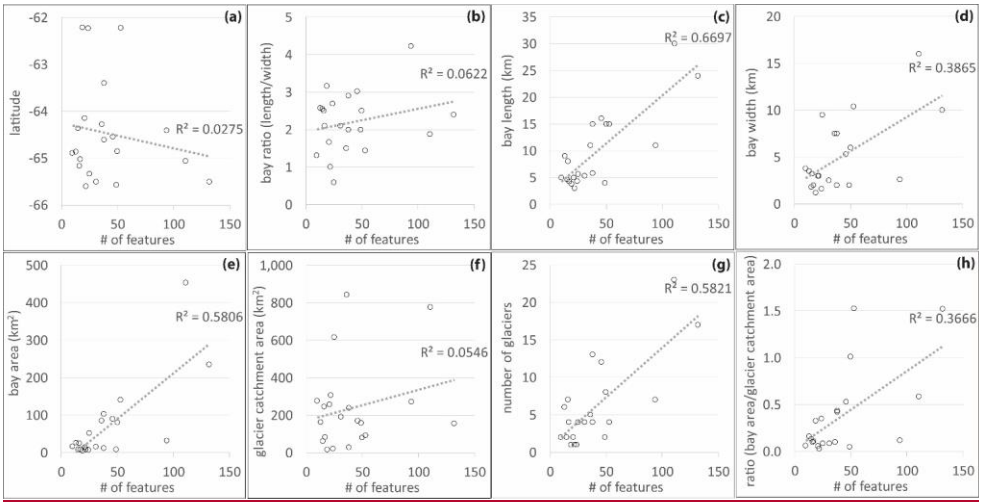

Figure 11. Graphs showing number of overall features found in the study areas as they relate to latitude, bay ratio, bay length, bay width, bay area, glacier catchment area, number of glaciers, and the ratio of bay area to glacier catchment area.

Deleted:

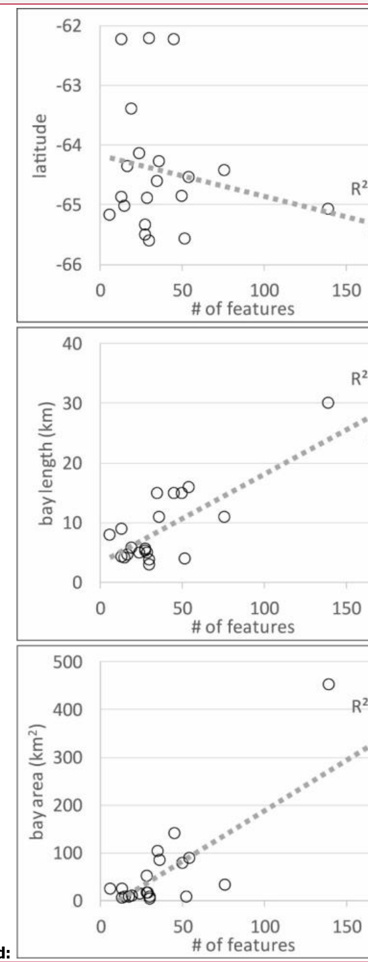

Formatted: Left, Keep with next

Deleted: ¶
Figure 11: Graphs showing number of overall features found in the study areas as they relate to latitude, bay ratio, bay length, bay width, bay area, and glacier catchment area. ¶

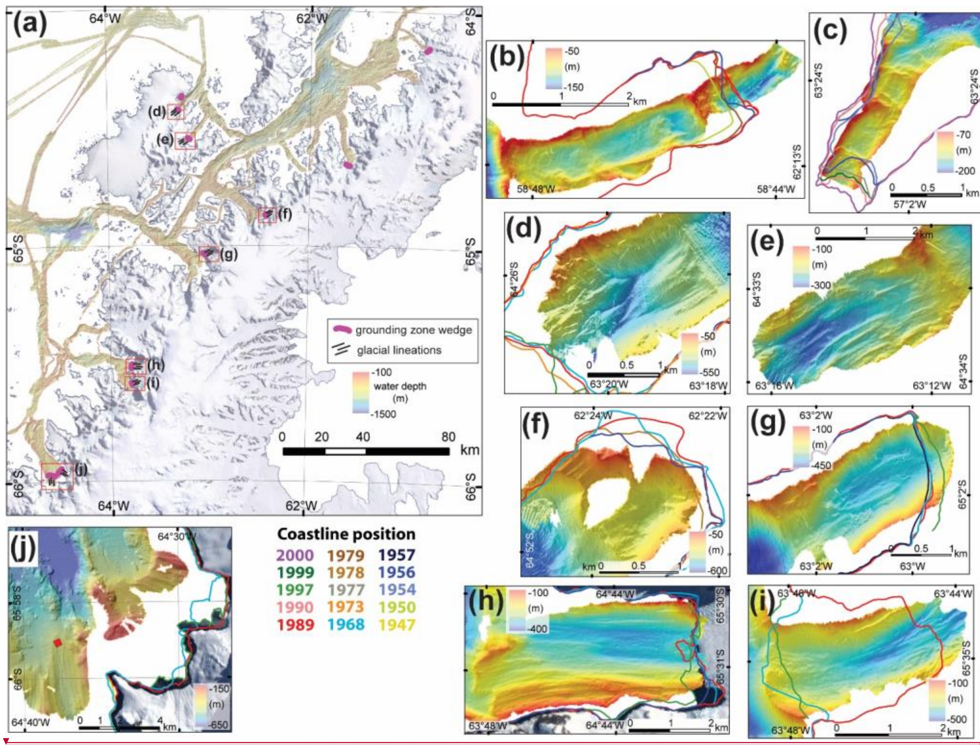

Figure 12. Map of the northwestern side of the Antarctic Peninsula (a) and features in the inner bays (Figs. b-j). Figures (b) Marian Cove and (c) Hope Bay are not in map (a), for location refer to Fig.1. Barilari Bay (j) from Christ et al. (2014) shows the proximal grounding zone wedge and glacial lineations; the red square shows the location of sediment core collected in 2010 and used for chronology in Christ et al. (2014). Coastline positions from Cook et al. (2014).

Deleted:

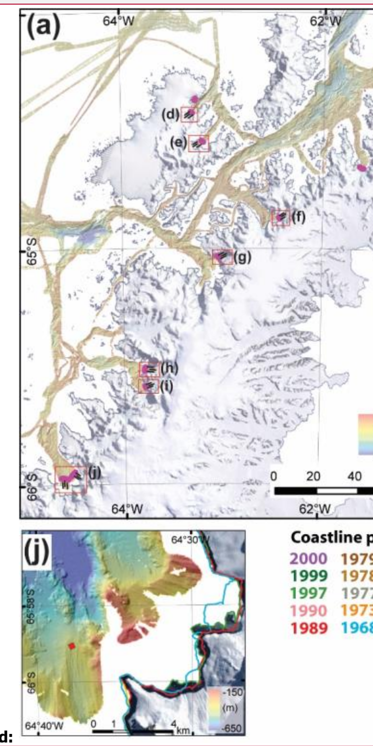

Formatted: English (United States)

Formatted: Caption, Left

Deleted: ¶

Figure 12: Map of central Antarctic Peninsula (a) and features in the inner bays (Figs. b-j). Figures (b) Marian Cove and (c) Hope Bay are not in map (a), for location refer to Fig.1. Barilari Bay (j) from Christ et al. (2014) shows the proximal grounding zone wedge and flutings, the red square shows the location of sediment core collected in 2010 and used for radiocarbon dating in Christ et al., (2014).¶

Table 1. Geomorphic features mapped and criteria for identification

Glacial landform	Defining characteristics	Dimensions min-max (meters) length, width, height	Formation interpretation	Example
Crevasse squeeze ridge	Small, short ridges, cross cutting each other or isolated	30-300, 10-30, 1-3	Depositional, form in crevassed glacier terminus	Fig. 6g
Moraine	Transverse ridge, found individually or amalgamated	250-1000, 100-300, 8-30	Depositional, form in front of glacier terminus during short episode of ice stability	Fig. 6g
Grounding zone wedge	Transverse ridge, wedge shaped, steep distal and gentler proximal side	800-8000, 80-2500, 10-130	Depositional, form in front of glacier terminus during long episode of ice stability	Fig. 6e
Glacial lineation	Elongated, symmetric, parallel to semi-parallel ridge (to one another and to bay length)	80-2700, 5-200, 1-20	Depositional or erosional, form by ice ploughing	Fig. 6a
Drumlin	Tear-drop shaped with tail, formed in deformable sediment	500-1200, 60-380, 5-30	Depositional or erosional, form in glacigenic sediment	Fig. 6c
Crag-and-tail	Tear-drop shaped or large bedrock protrusion with tail, parallel to semi-parallel (to one another and to bay length)	130-900, 40-300, 2-28	Depositional or erosional, form in till or bedrock	Fig. 6d
Streamlined feature	Elongated hill formed in bedrock, symmetric to asymmetric	260-5000, 130-1200, 8-220	Erosional, form in bedrock	Fig. 6b
Meltwater channel	Linear to sinuous channels, formed in bedrock or sedimentary unit, found individually or in networks, abrupt initiation and termination points	270-7000, 8-800, 1-120	Erosional, form in bedrock or sedimentary units	Fig. 6d